
Proceedings of the International Symposium MISASA-IX
"Understanding the Martian System Through Biosignatures, Surface Processes, and Internal Dynamics"
February 26 – 27, 2026 @ St. Palace Kurayoshi
IPM
J-PEAKS

Symposium Program & Oral Presentations

Day-1 (Feb 26)

10:00-10:15 Opening statement from IPM Director

10:15-11:45 Keynote talks

10:15-10:45 Janice L. Bishop (SETI Institute/NASA Ames Research Center)
"Constraining Past Geochemical Environments on Mars Through the Mineral Record" (→p4)

10:45-11:15 Shino Suzuki (RIKEN)
"A Rock–Water Interaction–Driven Biosphere: Implications as a Mars Analog" (→p5)

11:15-11:45 Taichi Kawamura (IPGP, Univ. Paris Cité)
"Mars Internal Structure as seen by InSight and Implication for Future Seismic Observation of Mars" (→p6)

11:45 – 13:30 Lunch

13:30 – 13:45 Greeting from Okayama University President

13:45 – 14:30 J-PEAKS research projects

13:45-14:00 Institute of Plant Science and Resources (Hisashi Hisano)
14:00-14:15 Research Institute for Interdisciplinary Science (Sayuri Takatori)
14:15-14:30 Institute for Planetary Materials (Jun Kameda/Trishit Ruj)

14:45 – 16:05 Internal Dynamics & Future Mars Missions

14:45-15:05 Yuki Harada (Nagoya Univ.)
"Martian Electromagnetism: From Space Environment into the Interior of Mars" (→p7)

15:05-15:25 Takuto Minami (Kobe Univ.)
"Probing the Martian Interior Using Electromagnetic Methods" (→p8)

15:25-15:45 Yasuhito Sekine (ELSI, Science Tokyo)
"Warming early Mars by a return of hydrogen from the core" (→p9)

15:45-16:05 Tomohiro Usui (ISAS, JAXA)
"JAXA's Stepwise Mars Landing Exploration Program" (→p10)

16:20 – 17:40 Astrobiology

16:20-16:40 Yasunori Hori (Okayama Univ.)
"Toward the Detection and Characterization of Habitable Earth-sized Planets" (→p11)

16:40-17:00 Adam Corbett (IPM, Okayama Univ.)
"Aldehyde hydration controls radical reaction pathways during parent body aqueous alteration" (→p12)

17:00-17:20 Michael Rowe (Univ. Auckland)
"Gallium in silica as a potential new type of biosignature for past life on Mars" (→p13)

17:20-17:40 Maxwell Craddock (ELSI, Science Tokyo)
"Laboratory Simulations of Organic Synthesis in Enceladus: An Integrated Laboratory-Mission Perspective on Habitability" (→p14)

17:40 – 19:00 Poster session

19:00 – Banquet at Champagne room (4F)

Day-2 (Feb 27)

9:00-10:20 Surface geology

9:00-9:20 Hitoshi Hasegawa (Kochi Univ.)
"Deciphering the evolution of aqueous environment on Mars: Geomorphological perspectives" (→p15)

9:20-9:40 Yoshinori Kodama (Tottori Univ.)
"A comparative study of windward slope gradients of transverse dunes on Mars and Earth" (→p16)

9:40-10:00 Yoshiko Ogawa (Univ. Aizu)
"Integrated Spectral Analysis and Web-GIS/VR System Development for Mars" (→p17)

10:00-10:20 Makiko Ohtake (IPM, Okayama Univ.)
"Estimated Lunar Mantle Composition by SLIM Multiband Camera" (→p18)

10:40 – 11:40 Instrument Developments

10:40-11:00 Yasushi Takahashi (Okayama Univ.)
"Compact Spacecraft Potential Sensor Using Charge-Induced Optical Absorption in a Silicon Photonic Waveguide" (→p19)

11:00-11:20 Kazuto Saiki (Ritsumeikan Univ.)
"Why Did Our Lunar Near-Infrared Spectral Cameras Take This Design? — The Development History of Spaceborne Instruments with Potential Relevance to Mars Exploration —" (→p20)

11:20-11:40 Yusuke Nakauchi (Ritsumeikan Univ.)
"Development of VIS–NIR Multi-band and Hyperspectral Imaging Instruments for Lunar and Mars Landing Missions" (→p21)

11:40 – 12:00 Closing statement & Announcement

12:00 – 13:00 Lunch

13:30 – 15:30 IPM Laboratory Tour (see Event section)

Poster Presenter List (A-Z)

- Hiral Bijoy (IPM, Okayama Univ.) "From Preservation to Sublimation: Ice Stability in Martian Mid-Latitude Craters" (→p22)
- Zhiyuan Chen (IPM, Okayama Univ.) "Effect of iron content on viscosity of ringwoodite and its implication for the rheology of the Martian mantle" (→p23)
- Takumu Chijiiwa (IPM, Okayama Univ.) "Habitability at high Martian latitudes explored by remote sensing, field surveys, and experiments" (→p24)
- Dilan H. F. Diyalanthonige (IPM, Okayama Univ.) "The Effect of Water on Martian Magma Ocean Evolution: Experimental Insights into dense silicate layer at the CMB" (→p25)
- Kumpei Goromaru (Kochi Univ.) "Terrain Classification on Saturn's Moon Titan by Machine Learning (Preliminary Result)" (→p26)
- Maya Hamaguchi (IPM, Okayama Univ.) "Development of an analytical strategy to determine the compound and position-specific isotope values of non-derivatised extraterrestrial amino acids" (→p27)
- Jinze He (IPM, Okayama Univ.) "P-V-T equation of state of calcium ferrite-type $CaAl_2O_4$ up to 25 GPa and 1500 K by using a multi-anvil press and in-situ synchrotron X-ray diffraction" (→p28)
- Daijo Ikuta (IPM, Okayama Univ.) "Sound velocity measurements of iron alloys by inelastic x-ray scattering and the implications for planetary interiors" (→p29)
- Takayuki Ishii (IPM, Okayama Univ.) "Sound velocities of ringwoodite and majorite garnet: Implications for Martian mantle seismic profiles" (→p30)
- Dongliang Jiang (Zhejiang University) "Experimental Investigation of Martian Mantle Mineral Phase Transitions under High Pressure and High Temperature Conditions" (→p31)
- Matthew Izawa (IPM, Okayama Univ.) "A First Look at Reflectance Spectrum of Ringwoodite: Opening a New Window to shock Metamorphism and Deep Mantle Processes on Extraterrestrial Bodies" (→p32)
- Hiroshi Kitagawa (IPM, Okayama Univ.) "Carbonate Melts in the Lithosphere-Asthenosphere Boundary: Geochemical Evidence from Ultramafic Xenoliths in an Oceanic Island" (→p33)
- Ren Kito (IPM, Okayama Univ.) "Hydrology on Ancient Mars Derived from Morphologies and Tank Experiments od Deltas" (→p34)
- Nozomi Kondo (IPM, Okayama Univ.) "Tetrahedral symmetry breaking in albite-anorthite glass structures related to Aluminum atom: Possible origin of viscosity difference in plagioclase melts" (→p35)

- Nurcan Kucukarslan (Chiba Institute of Technology) “Searching for the clues about the early iron history in Central Anatolia” (→p36)
- Tak Kunihiro (IPM, Okayama Univ.) “Mineralogical Hosts of Be and B in Ryugu: In Situ Ion Imaging Constraints” (→p37)
- Takuya Moriguti (IPM, Okayama Univ.) “Systematic investigation of matrix effects in SIMS lithium isotope analysis: Constraints from the compositional dependence of in-house silicate standards” (→p38)
- Keisuke Onodera (IPM, Okayama Univ.) “Recent Progress in Lunar Seismology: Discovery of Repeating Shallow Moonquakes in the Apollo Lunar Seismic Data” (→p39)
- Tsutomu Ota (IPM, Okayama Univ.) “Habitability of boron-rich environment in ancient sea; Insights from tourmaline in a mesoarchean pelagic hydrothermal system” (→p40)
- Natalia Pravikova (Lomonosov Moscow State Univ.) “Geochemical and isotopic characteristics of the Magnitogorsk and Ui River Zones’ Early Carboniferous volcanic complexes (Southern Urals, Russia)” (→p41)
- Takaki Sako (IPM, Okayama Univ.) “Reconstructing the Martian Surface Environment Through Polygonal Patterned Ground” (→p42)
- Karin Sugiura (Kochi Univ.) “Exploring the aqueous environmental history of Eridania Basin on Mars” (→p43)
- Hyu Takaki (IPM, Okayama Univ.) “Infiltration of Fe-S Melt into Ilmenite: Implications for the Lunar Low-Velocity Zone” (→p44)
- Yoshinori Takano (JAMSTEC) “Method development of novel organic-inorganic interface molecules in the Solar System: Optimization and perspectives of hybrid cross-separation with high-resolution mass spectrometry” (→p45)
- Sayuri Takatori (RIIS, Okayama Univ.) “Development of a Vacuum Ultraviolet Laser System for Thorium-229 Nuclear Clock” (→p46)
- Kazuki Yamanaka (SOKENDAI) “Cryogenic Evaluation of Magnetic Field Characteristics in a Velocity-Type Passive Seismometer” (→p47)
- Chia-Yu Yang (Kyoto Prefectural Univ.) “Climate control on Cr and Ni bioavailability in ultramafic soils along an elevation gradient in Mt. Kinabalu, Malaysia” (→p48)
- Takashi Yoshino (IPM, Okayama Univ.) “Effect of Fe on electrical conductivity of wadsleyite: implications for conductivity structure of deep Martian mantle” (→p49)

Location of Poster Boards

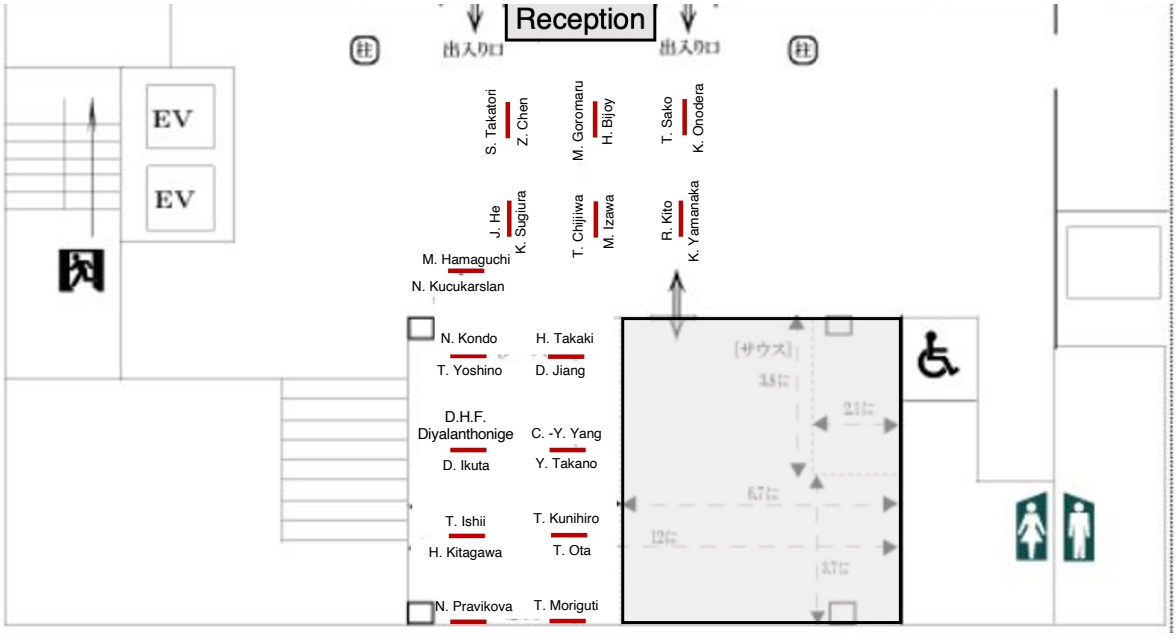

CONSTRAINING PAST GEOCHEMICAL ENVIRONMENTS ON MARS THROUGH THE MINERAL RECORD

J. L. Bishop[1],

[1] SETI Institute & NASA Ames Research Center (339 Bernardo Avenue, Suite 200, Mountain View, CA 94043, USA; jbishop@seti.org).

Investigation of minerals on Mars provides an opportunity to evaluate the geochemical environments in which they formed. The CRISM imaging spectrometer collected near complete global coverage at lower resolution plus thousands of higher resolution targeted images across the planet that have revolutionized our understanding of the surface mineralogy and geochemical evolution of Mars [1]. Comparing changes in alteration mineral assemblages on Mars with observations from the field and lab provides information about changes in mineralogy on Mars as well as transitions in the early martian environment and climate [e.g., 2,3,4]. Recent investigations by the Curiosity and Perseverance rovers have revealed small outcrops of unique minerals that extend our understanding of the mineralogy determined from orbit. Observation of inverse abundances of siderite and sulfates at Gale crater could have implications for the martian atmosphere [5] and interactions of phyllosilicates, carbonates, sulfates, and iron oxides/hydroxides could be linked to environmental transformations on early Mars [6]. Evidence of redox reactions at Jezero crater point towards intriguing chemical reactions that could represent prebiotic chemistry [7]. Coordinating orbital and in situ data from Mars with laboratory and field experiments provides context for understanding implications for redox reactions in minerals on Mars [8].

References: [1] Murchie S. L. et al. (2019) in: Remote Compositional Analysis …, Cambridge University Press, 453-483. [2] Bishop J. L. et al. (2018) Nature Astronomy, 2, 206-213. [3] Bishop J. L. et al. (2020) Icarus, 341, 113634. [4] Wordsworth R. et al. (2021) Nature Geoscience, 14, 127-132. [5] Tutolo B. M. et al. (2025) Science, 388, 292-297. [6] Bishop J. L. & Lane M. D. (2025) Science, 388, 251-252. [7] Hurowitz J. A. et al. (2025) Nature, 645, 332-340. [8] Bishop J. L. & Parente M. (2025) Nature, 645, 317-318.

A ROCK–WATER INTERACTION–DRIVEN BIOSPHERE: IMPLICATIONS AS A MARS ANALOG

S. Suzuki[1]

[1] Geobiology and Astrobiology Laboratory, PRI, RIKEN, 2-1 Hirosawa, Wako, Saitama 351-0198, Japan, shino.suzuki@riken.jp

NASA's Mars exploration program has been guided by the principle "Follow the water," recognizing liquid water as a key indicator of planetary habitability. Geological evidence suggests that surface water existed on Mars approximately 3.7–3.0 billion years ago, although liquid water is absent under present surface conditions. If subsurface liquid water reservoirs persist, an important question is whether life could survive over geologic timescales in long-term isolated environments.

To address this question, we investigated microbial ecosystems in the Kidd Creek Mine (Canadian Shield), where fracture waters have been isolated for over one billion years. Microbial analyses revealed low species diversity, yet metabolically active microorganisms were clearly present. These ecosystems were independent of photosynthesis and sustained by geochemically derived energy from water–rock interactions. Hydrogen produced by radiolysis and serpentinization functioned as a primary electron donor, while sulfate formed through sulfide mineral oxidation served as an electron acceptor, supporting anaerobic metabolisms such as sulfate reduction. Methane and other light hydrocarbons were also present at elevated concentrations and may have provided additional energy sources. Although free molecular oxygen was largely absent, radiolytically generated reactive oxygen species may have produced trace amounts of O_2.

These results indicate that persistent redox disequilibria can sustain microbial life in long-term isolated subsurface environments. Electron flux driven by water–rock interactions may represent a fundamental energy basis for deep biospheres and provides important insight into potential Martian subsurface habitability.

In addition, we will discuss planetary protection requirements mandated under Article IX of the 1967 Outer Space Treaty and implemented through COSPAR planetary protection policy in the context of Mars exploration. We will also introduce the development of an ultra-compact MALDI-TOF mass spectrometer being advanced as a candidate science payload for future life-detection missions.

Mars Internal Structure as seen by InSight and Implication for Future Seismic Observation of Mars

T. Kawamura[1]

[1] Université Paris Cité, Institut de Physique du Globe de Paris, CNRS, Paris, France (kawamura@ipgp.fr)

NASA's InSight mission successfully landed on Mars in 2018 and conducted four years of seismic monitoring. InSight was equipped with the most sensitive broadband seismometer ever deployed for another planet, the Very Broad Band (VBB) instrument. Its high sensitivity enabled detailed seismic investigations despite the limitation of having only a single seismic station.

InSight detected approximately 1,300 Marsquakes, which have been used to investigate the planet's internal structure and to establish a reference seismic model as well as characterize Martian seismicity. A major milestone was the establishment of the first one-dimensional seismic model of Mars, providing quantitative constraints on crustal thickness, mantle structure, and the core–mantle boundary depth [1–3]. This model has since become a reference framework in Martian geophysics. The core structure has subsequently been revisited following the detection of core-transiting phases (e.g., SKS)[4], core-grazing phases (e.g., Pdiff) suggesting a basal molten silicate layer[5], and the discovery of a ~600-km solid inner core via reflected phases[6]. These results indicate that significant amounts of light elements are required to explain the core density.

Another major topic concerns the presence of water in the Martian crust and upper mantle. Several studies have suggested that the mid-crust may be water-saturated based on the Vp/Vs ratios inferred from InSight data[7, 8]. However, this interpretation remains debated. The relatively low seismic attenuation observed in the Martian crust appears inconsistent with a fully water-saturated environment. Alternative models therefore propose mechanisms such as viscous pore closure and a more limited distribution of water held in hydrated minerals[9].

I will conclude by reviewing the remaining open questions following the InSight mission and their implications for future planetary seismic investigations.

References: [1] Khan, A. *et al.*(2021) *Science* **373**, 434–438 [2] Knapmeyer-Endrun, B. *et al.* (2021) *Science* **373**, 438–443 [3] Stähler, S. C. *et al.* (2021) *Science* **373**, 443–448 [4] Irving, J. C. E. *et al.* (2023) *Proceedings of the National Academy of Sciences* **120**, e2217090120 [5] Samuel, H. *et al.* (2023) *Nature* **622**, 712–717 [6] Bi, H. *et al.* (2025) *Nature* **645**, 67–72 [7] Wright, V., Morzfeld, M. & Manga, (2024) *Proceedings of the National Academy of Sciences* **121**, e2409983121 [8] Katayama, I. & Akamatsu, Y., (2024) *Geology* **52**, 939–942 [9] Knapmeyer-Endrun, B. *et al. Physics of the Earth and Planetary Interiors* **366**, 107383 (2025).

Martian Electromagnetism: From Space Environment Into the Interior of Mars

Y. Harada[1], T. Minami[2], and M. Sato[3],

[1] Institute for Space–Earth Environmental Research, Nagoya University, Furo-cho, Chikusa-ku, Nagoya 464-8601 Japan (harada.yuki.i6@f.mail.nagoya-u.ac.jp), [2] Kobe University (tminami@port.kobe-u.ac.jp), [3] Tokyo University of Science (msato@rs.tus.ac.jp).

Magnetic field structures in the near-Mars space are primarily formed by electric currents resulting from the solar wind interaction with the upper atmosphere and crustal magnetic fields of Mars [1]. Recent studies revealed that ionospheric dynamo currents driven by neutral winds in the thermosphere (analogous to the S_q ionospheric currents at Earth) also contribute to shaping the Martian magnetic field environment [2,3]. These magnetospheric and ionospheric current systems not only represent a close coupling between the outer "spheres" (*i.e.*, the solar wind, magnetosphere, ionosphere, and neutral upper atmosphere) but also serve as external sources of time-varying magnetic fields imposed upon the interior of Mars. The temporal variations in external magnetic fields induce electric currents within the Martian interior, which in turn generate "induced" magnetic fields that are observable on the surface and in orbit of Mars. Electromagnetic induction has been utilized to probe the electrical conductivity structure of Earth's interior and can be applied to the interior of Mars in principle, provided that appropriate measurements are conducted. Since the electrical conductivity of the interior can be used to infer relevant physical and chemical properties, electromagnetic induction studies provide powerful tools to obtain valuable information on planetary internal structures, partly achieved by using satellite magnetic data with periods longer than a day [4]. However, studies based on magnetic measurements at the Martian surface are crucial for revealing shallow crustal structures, including potential liquid water in cracks, and structural heterogeneity from the crust to the upper mantle, as expected from Martian internal tectonic processes. Since standard magnetotelluric sounding is not readily available at Mars, given the difficulty of burying and installing electrodes for electric field measurements by a resource-limited landing mission, alternative methods using only magnetic field measurements have been proposed [5]. One of the critical challenges for planning and applying such magnetometer-only methods at Mars is that our knowledge about the external field sources (*i.e.*, magnetospheric and ionospheric currents) is very limited. We do not yet fully understand a global-scale, steady-state system of magnetospheric and ionospheric currents at Mars, let alone local structures and temporal variability thereof. Here, we provide a brief review of past and ongoing efforts to elucidate the Martian current systems utilizing currently available observational data and numerical models.

References: [1] Ramstad, R. et al. (2020) Nat. Astron., https://doi.org/10.1038/s41550-020-1099-y. [2] Gao, j. et al. (2024) Nat. Commun., https://doi.org/10.1038/s41467-024-54073-9. [3] Harada, Y. et al. (2025) Sci Rep, https://doi.org/10.1038/s41598-025-24881-0. [4] Civet, F. and Tarits, P. (2014) Earth, Planets and Space, https://doi.org/10.1186/1880-5981-66-85. [5] Pincon, J. L. et al. (2000) Planet. Space Sci., https://doi.org/10.1016/S0032-0633(00)00108-2.

Probing the Martian Interior Using Electromagnetic Methods

T. Minami[1], S. Hoshino[2], Y. Harada[3], and M. Sato[4]

[1]Kobe University, 1-1 Rokkodaicho, Nada-ku, Kobe, 657-8501, Japan (tminami@port.kobe-u.ac.jp), [2] Kobe University (s.hoshino@stu.kobe-u.ac.jp), [3] Nagoya University (harada.yuki.i6@f.mail.nagoya-u.ac.jp), [4] Tokyo University of Science (msato@rs.tus.ac.jp).

While the internal structure of Mars has been primarily constrained by seismic observations, electromagnetic methods that probe the planet's electrical resistivity offer significant potential to advance our understanding of the Martian interior. Electrical resistivity is particularly sensitive to the presence of partial melts and water. Previous observational estimates of the Martian resistivity structure were only derived from magnetic observations at satellite altitude by the Mars Global Surveyor satellite [1], which inferred a global one-dimensional structure based on variations with periods longer than one day. Although that study suggested a high likelihood of of low-resistivity layer in the lower mantle, the resistivity structure at shallower depths, including the upper mantle and crust, and the possible presence of liquid water in the crust [2], remain unconstrained. Surface magnetic measurements could probably provide critical information to address these gaps.

Magnetic measurements at the Martian surface using multiple landers are currently planned as part of JAXA's STEP1 concept. Mars is known to have an ionosphere, which allows the plane-wave assumption and makes conventional magnetotelluric (MT) investigations feasible in principle [3]. However, MT surveys require electrodes to be deployed in the ground, which is not practical for unmanned rover missions. Alternatively, subsurface resistivity sounding by using only magnetic field observations remains a promising approach. Methos such as the Geomagentic Depth Sounding method, which assumes a source source geometry; the Horizontal Spatial Gradient method, which uses simultaneous measurements at more than two sites; and the induction vector analysis can be candidates in the future mission. Recently, magnetic data from the InSight mission [3] have provided an excellent opportunity to test these approaches. Our induction vector analysis suggests the presence of lateral resistivity contrasts beneath the InSight landing site, consistent with the mantle plume hypothesis in Elysium Planitia proposed in previous studies [3].

In addition, magnetic measurements obtained not only at the Martian surface but also at varying altitudes during descent offer a unique opportunity to constrain crustal remanent magnetization and its thickness. In particular, magnetic anomalies associated with impact craters can provide insights into the state of Martian dynamo at the time of crater formation. Recent studies suggest that the Martian dynamo may have persisted into the Hesperian era [5]. Therefore, magnetic measurements at and near the Martian surface within craters with well-constrained geological ages have strong potential to clarify the evolutional history of Martian dynamo.

References: [1] Civet, F. and Tarits, P. (2014) Earth, Planets and Space, https://doi.org/10.1186/1880-5981-66-85. [2] Katayama, I., and Akamatsu, Y. (2024) Geology, https://doi.org/10.1130/G52369.1. [3] Mittelholz, A., et al. (2023) J. Geophys. Res.: Planets, https://doi.org/10.1029/2022JE007616. [4] Broquet, A., and Andrews-Hanna, J. C. (2023). Nat. Astro., https://doi.org/10.1038/s41550-022-01836-3. [5] Mittelholz, A. et al. (2020) Sci. Adv., https://doi.org/10.1126/sciadv.aba0513.

Warming early Mars by a return of hydrogen from the core

Y. Sekine[1], T. Hirai[1], R. Wordsworth[2], and K. Hirose[3],

[1] Earth-Life Science Institute, Institute of Science Tokyo, Tokyo, Japan (sekine@elsi.jp), [2]School of Engineering and Applied Sciences, Harvard University, Cambridge, Massachusetts, USA, [3] Department of Earth and Planetary Science, The University of Tokyo, Tokyo, Japan

Many lines of geological and geochemical evidence indicate the existence of surface liquid water for geological time periods (e.g., ~1–10 Myrs) on early Mars [e.g., 1, 2]. The surface temperature during the wet periods may have reached 30–40 °C in maximum in order to form crystallized Al-rich clay minerals [2]. The occurrence of the surface water seems to be concentrated at 3.8 billion years ago (3.8 Ga), around the boundary of the Noachian and Hesperian periods [e.g., 1]. Previous studies attempted to explain the occurrence of transient (~1 Myr-long) wet conditions by stochastic geological events, such as large asteroidal impacts and volcanic eruptions [3]; however, no studies have explained the concentration of warm and wet periods at around 3.8 Ga. Furthermore, high surface temperatures, such as 30–40 °C, may be also hard to be achieved on early Mars in the stochastic geological events.

Here, we propose a new scenario to make Mars warm both intensively and episodically in a certain period (0.1–1 Gyrs) of time after the formation. Mars metallic core, with the high abundances of H and S [4], would have segregated upon cooling of the interior, accompanying with the disappearance of magnetic field (~4.2–4.1 Ga). The core segregation may have resulted in the occurrence of a H-rich Fe melt (Fe-H) layer in the outer region of the core [5]. Through the exchange of H between the Fe-H layer and basal magma in the mantle [4], the density of the basal magma would have gradually become lighter over time, finally leading to upwelling of the basal magma due to the buoyancy. Our calculations show that when the Fe-H layer is enriched in H about 4–5 times that of the initial core owing to the core segregation at 2000 K of the core-mantle temperature, the basal magma can be upwelled in the mantle due to the buoyancy. This upwelled basal magma contains ~0.7 wt.% of total H due to a supply from the core.

A part of the upwelled magma may have erupted on the surface, degassing a large amount of H_2 and, consequently, warming the surface intensely for a geological time. The upwelled basal magma, if occurred, should be highly enriched in Fe compared with Mg [6] and may have formed a flat plain, e.g., flood basalt, owing to its high temperatures. The findings of Fe-rich igneous rocks in the northern basalt plain of current Mars by the Perseverance Rover [7] are consistent with our scenario. The InSight Lander finds a discontinuity in several km depth within the crust of the northern hemisphere [8]. Assuming this discontinuity as a flood basalt layer of the basal magma eruption with total H (a sum of H_2 and H_2O) for upwelling, we can estimate a released H_2 partial pressure in the atmosphere after the eruption as 0.5–1.0 bar. Without any other greenhouse effect gases, the surface temperature can reach as high as 50–150 °C depending on the H_2 abundance. Warm climates, with temperatures higher than the freezing point of water, can be sustained for 1–4 Myrs after the eruption. The temperature higher than 100 °C may not be consistent with the presence of extensive smectite on Mars given the conversion of smectite to talc at the high temperatures. However, Al-rich clay may need a relatively high temperature, such as 30–50 °C, sustaining for ~1 Myrs [2], which is achieved in our calculation when 0.5 bar of H_2 erupted onto the surface. The high levels of H_2 in the atmosphere, in turn, would have reduced atmospheric CO_2 into CO during the warm period, possibly preventing extensive deposition of carbonate minerals on the surface.

References: [1] Ehlmann et al. (2011) Nature. 479, 53. [2] Bishop et al. (2018) Nat. Astron. 2, 208. [3] Wordsworth et al. (2017) Nat. Geosci. 14, 127. [4] Khan et al. (2023) Nature 622, 718. [5] Yokoo et al. (2022) Nat Commun. 13, 644. [6] Elkins-Tanton et al. (2005) JGR Planets 110, E12S01, [7] Liu et al. (2022) Science 377, 1513. [8] Knapmeyer-Endrun et al. (2021) Science 373, 438.

JAXA'S STEPWISE MARS LANDING EXPLORATION PROGRAM

T. Usui[1]
[1] Japan Aerospace Exploration Agency (3-1-1 Yoshinodai, Sagamihara, Kanagawa 252-5210, Japan; usui.tomohiro@jaxa.jp)

JAXA is formulating a stepwise Mars landing exploration program under Japan's Basic Plan on Space Policy [1], aiming to provide compact yet capable access to science-driven landing sites across the Martian surface, including polar and highland regions. The program seeks to achieve high-priority scientific outcomes defined by the planetary science community while acquiring key technologies required for the Artemis Moon-to-Mars strategy. It is also designed to expand collaboration with industry and universities, consistent with broader policy goals of extending human activity beyond Earth.

JAXA's space exploration roadmap [2] targets a rover-based Mars landing mission around 2040 through this stepwise program. The program builds upon the Martian Moons eXploration (MMX) mission in the late 2020s and proceeds through three landing missions in the 2030s. The scientific objectives evolve systematically: MMX addresses the origin, transport, and supply of water in the Mars system; Step-1 investigates atmospheric and interior dynamics; Step-2 focuses on water reservoirs, escape processes, and material cycling; and Step-3 ultimately aims to explore habitability and the possible existence of Martian life. The program is closely coupled with engineering development and integrated into JAXA's broader exploration roadmap [2]. Synergies are anticipated with JAXA's lunar exploration missions (e.g., SLIM and LUPEX), deep-space orbital transfer vehicle (OTV) concepts, and the progressive use of communication and navigation constellations.

Mars exploration is entering a profound transition from stand-alone science missions to programmatic exploration that integrates scientific and policy objectives. The proposed Mars landing exploration program therefore represents a unique community-driven initiative and can serve as a pathfinder for a new model of international exploration in the Artemis Moon-to-Mars era.

REFERENCES

[1] Basic Plan on Space Policy (in Japanese) [link]
[2] Japan's Proposed International Space Exploration Scenario (in Japanese) [link]

Toward the Detection and Characterization of Habitable Earth-sized Planets

Yasunori Hori[1,2],

[1] Okayama University, 3-1-1 Tsushima-naka, Kita-ku, Okayama 700-8530, Japan (yhori@okayama-u.ac.jp)
[2]Astrobiology Center, 2-21-1 Osawa, Mitaka, Tokyo 181-8588, Japan

Over the past thirty years, exoplanet surveys have revealed a diverse population of planets beyond the Solar System. Even Earth-sized planets have been discovered in the habitable zones of low-mass stars, such as Proxima Centauri b [1], Teegarden's Star b [2], and the TRAPPIST-1 system [3,4]. Observing the atmospheres of these potentially habitable planets helps us understand the diversity of terrestrial planets beyond the Solar System and can provide clues to the presence of biosignatures of life, such as methane and oxygen. The outstanding performance of the infrared spectrograph onboard the James Webb Space Telescope (JWST), together with the Hubble Space Telescope (HST), has led to significant progress in our understanding of the atmospheric chemistry of exoplanets. For instance, JWST observations of K2-18b [5], a Hycean planet candidate in the habitable zone, suggest that methane and carbon dioxide exist in its temperate atmosphere.

The achievement of extremely high precision radial-velocity measurements (~cm/s) and the launch of the planned PLATO mission and the Roman Space Telescope are expected to rapidly increase the number of promising Earth-sized planet candidates in the habitable zone. In addition, next-generation ground-based telescopes, such as the Thirty Meter Telescope, the Giant Magellan Telescope, and the European Extremely Large Telescope, are designed to perform high-contrast imaging of habitable Earth-sized planets. In the 2030s, further characterization of exoplanets, including their surface environments through reflected light observations (e.g., the detection of ocean glint, the vegetation red edge, and biofluorescence) and the detection of exomoons, will be key scientific goals in exoplanet research. These efforts will bring us closer to the discovery of life on an Earth-like planet beyond the Solar System.

In this talk, I will review the current status of astrobiology research in the field of exoplanetary science and discuss future prospects in the late 2020s and 2030s with a focus on habitable terrestrial planets around Sun-like stars.

References: [1] Anglada-Escudé, G. et al. (2016) Nature, 536, 7617, 437–440. [2] Zechmeister, M. et al. (2019) A&A, 627, A49, 14pp. [3] Gillon, M. et al. (2016) Nature, 533, 7602, 221-224. [4] Gillon, M. et al. (2017) Nature, 542, 7642, 456-460. [5] Madhusudhan, N. et al. (2023) ApJL, 956, L13, 16pp.

Aldehyde hydration controls radical reaction pathways during parent body aqueous alteration

A. G. Corbett[1*], T. Ota[1], M. Yamanaka[1], M. Hamaguchi[1], R. Tanaka[1], C. Potiszil[1]

[1] Pheasant Memorial Laboratory, Institute for Planetary Materials, Okayama University, Yamada 827, Misasa, Tottori, 682-0193, Japan.
*adam_corbett@s.okayama-u.ac.jp

Monocarboxylic acids are among the most abundant soluble organic materials across carbonaceous chondrites and the asteroids 162173 Ryugu and 101955 Bennu[1-2]. While considered to be major products of aldehyde oxidation during aqueous alteration events[3], trends in relative abundances of C_1-C_6 carboxylic acids indicate an energetic or kinetic preference for the survival and potential catalytic concentration of the shorter-chain formic and acetic acids. Here it is shown that aldehyde hydration equilibria in aqueous environments impose a fundamental control on radical reaction pathways during aqueous alteration. In aqueous solution, short-chain aldehydes exist predominantly in their hydrated gem-diol forms[4], which are effectively buffered against acyl radical formation and subsequent rapid chain-scission fragmentation pathways. Importantly, hydration suppresses fragmentation while still permitting oxidation through radical capture and dehydration pathways[5], allowing hydrated aldehydes to remain viable precursors to carboxylic acids. In contrast, longer-chain aldehydes increasingly favour the free carbonyl form in aqueous solution[4], enabling competition between direct oxidation and α-scission following radical initiation. Quantum chemical (DFT) calculations indicate that the α-scission barrier for the free C_2 radical is considerably higher than those of C_3-C_6 radicals across a variety of potential aqueous alteration temperatures. However, for C_3-C_6 radicals, the activation energy barriers show minimal dependence on aliphatic chain length. α-scission barriers are substantially lower than β-scission barriers across all relevant acyl radicals, leading to the conclusion that α-scission is the energetically preferable fragmentation pathway for free-form aldehyde radicals after carbonyl H-abstraction. Fragmentation of free aldehydes leads to irreversible carbon loss via CO elimination and the generation of shorter-chain alkyl radicals, which may later oxidise to C_{n-1} carboxylic acids. Aldehyde selectivity therefore arises in part through hydration-controlled access to destructive radical pathways. Modest differences in radical lifetimes are expected to integrate over prolonged aqueous alteration timescales, enabling selective preservation and oxidation of short-chain aldehydes relative to longer-chain homologues. This reaction framework links meteoritic carboxylic acid distributions with aqueous alteration chemistry and highlights hydration as a controlling process in meteoritic organic delivery to early planetary surfaces.

References

[1] Naraoka, H. et al. *Science* **379**, 789 (2023
[2] Glavin, D.P. et al. *Nat. Astron.* **9**, 199-210 (2025)
[3] Chimiak, L. & Eiler, J. M. *Geochim. Chosmochim. Acta* **379,** 1-16 (2024)
[4] Tilgner, A. et al. *Atmos. Chem. Phys.* **21**, 13483-13536 (2021)
[5] Salta, Z. et al. *J. Phys. Chem. A.* **128**, 1603-1614 (2024).

GALLIUM IN SILICA AS A POTENTIAL NEW TYPE OF BIOSIGNATURE FOR PAST LIFE ON MARS

M.C. Rowe[1], K.A. Campbell[1], B. Lyon[1], T. Kunihiro[2], A. Langendam[3], T. Ota[2], D. Stallard[1], E. Nersezova[1], P. Osmers[1], S. Ruff[4]

[1]University of Auckland – Waipapa Taumata Rau, School of Environment & Te Ao Mārama – Centre for Fundamental Inquiry, Auckland 1010, NZ (Michael.rowe@auckland.ac.nz), [2]Okayama University, Institute for Planetary Materials, Misasa, Tottori 682-0193, Japan, [3]Australian Synchrotron Facility (ANSTO), Clayton, VIC 3168, Australia, [4]School of Earth and Space Exploration, Arizona State University, Tempe, AZ, 85287, USA.

Conclusive evidence of extraterrestrial life will require a high degree of verification, utilising multiple independent techniques. This is even more challenging when investigating ancient life, where we are limited to the geologic record, and organic biosignatures may have long since broken down. The trace element gallium has recently been identified associated with silicified microbial material in hot springs silica (sinter; Fig. 1)[1] in environments interpreted as analogous to those on early Mars (such as the silica deposits discovered by the NASA *Spirit* rover at Home Plate, Gusev Crater)[2]. However, it is unclear whether this striking gallium enrichment is the result of a metabolic process, or an abiotic side effect of silicification. The mechanism by which gallium is enriched is important to determining the utility of this potential biosignature. Gallium in its most common ionic form (Ga^{3+}) has an ionic radius and electronegativity similar to Fe^{3+}, which is commonly utilised by microbes for metabolic processes. It is therefore possible that Ga^{3+} is enriched accidentally, as a byproduct of Fe^{3+} utilisation. It has also been suggested recently that gallium enrichment is an abiotic process, linked instead to precipitation of silica oligomers which are more likely to bond to gallium as opposed to larger Si ring structures (colloidal silica)[3]. Enrichment of gallium in filamentous microbial sheaths then would result from preferential physico-chemical incorporation of the smaller silica oligomers in microbial sheaths, unrelated to microbial metabolism. To better understand the mechanisms of gallium enrichment we have investigated both the chemical structure (valence state, coordination number) of gallium in silica and whether there is evidence of gallium isotopic fractionation associated with enrichments in silicified microbial material. We have utilised recent to sub-recent hot spring sinter from New Zealand (Taupo Volcanic Zone) and Chile (El Tatio) – both regions that have many textural similarities to hydrothermal silica deposits at Home Plate, Mars [1,2].

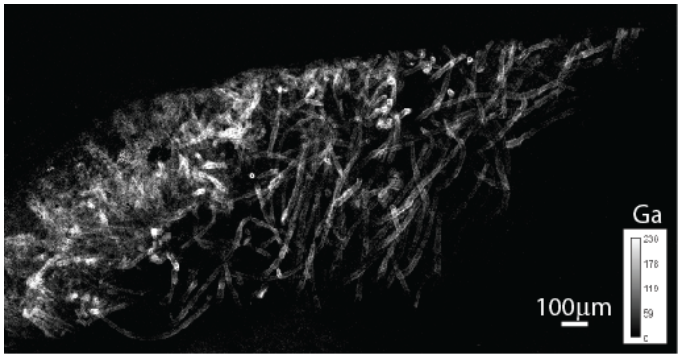

Figure 1: Gallium distribution in microbial filament sheaths from hot spring sinter at El Tatio, Chile. Analyzed by synchrotron XRF.

Gallium XANES (X-ray Absorption Near Edge Spectroscopy) analyses were conducted at the Australian synchrotron to examine whether enriched gallium in microbial sheaths has a change in coordination conditions (primarily tetrahedrally-coordinated with silica) that may indicate evidence of the formation of gallium–organic ligand bonds. All measurements of gallium XANES associated with microbial textures demonstrate gallium is tetrahedrally-coordinated, identical to gallium in high temperature (inferred abiotic) hydrothermal silica. This result suggests there is no evidence of Ga bound to organic components while silicified in the microbial sheaths. In this case, we define the new term "chemofabric" - the distribution of inorganic chemical components in unique textures that describe the interaction of various components to create the overall structure of the rock, as an analogous term to "biofabric". However, in situ gallium isotopes measured by the Cameca 1280 ion probe at the Institute for Planetary Materials (Misasa, Okayama University) indicates an isotopic fractionation of ~ 4‰ between silicified microbial filament sheaths enriched in gallium and adjacent (non-filamentous) silica. The lighter isotopic signature (more ^{69}Ga) in the silicified filament sheaths is consistent with the preferential utilisation of lighter isotopes for metabolic efficiency – however additional mechanisms exist for the preferential enrichment of lighter isotopes and are presently under investigation. In terms of the strength of the evidence for life, potential metabolic byproducts are viewed more favourably than textures (chemofabrics) alone. Ongoing technique development and analytical work (isotopic and chemical structure) on terrestrial sinters and microbial growth experiments will allow us to further refine models for microbial gallium enrichment in this important geologic setting for past, and perhaps even origin of, life.

References: [1] Nersezova E.E. et al. (2024) Chem Geo., 661, 122194. [2] Ruff S.W. and Farmer J.D. (2016) Nat. Commun., 7, 13554. [3] Lyon B. et al (2026) GCA (in press).

Laboratory Simulations of Organic Synthesis in Enceladus: An Integrated Laboratory-Mission Perspective on Habitability

Craddock M. L.[1]*, Sekine Y.[1,2,3], Napoleoni M.[4], Khawaja N.[5,4], Tan S.[6], Li Y.[7], Yang Z.[1], Sánchez L. H.[4], Yi R.[8], Postberg F.[4]

[1] Earth-Life Science Institute (ELSI), Institute of Science Tokyo, Japan, *craddockm@elsi.jp, [2]Institute of Nature and Environmental Technology, Kanazawa University, Japan, [3]Planetary Plasma and Atmospheric Research Center, Tohoku University, Japan, [4]Freie Universität Berlin, Institute of Geological Sciences, Germany, [5]Institute of Space Systems, University of Stuttgart, Germany, [6]Super-cutting-edge Grand and Advanced Research (SUGAR) program, Institute for Extra-cutting-edge Science and Technology Avant-garde Research (X-star), Japan Agency for Marine-Earth Science and Technology (JAMSTEC), Japan, [7]School of Earth and Space Sciences, University of Science and Technology of China, China, [8]State Key Laboratory of Deep Earth Processes and Resources, Guangzhou Institute of Geochemistry, Chinese Academy of Sciences, China

Recent Cassini observations of Enceladus' plume and Saturn's E ring have revealed a diverse inventory of organic compounds, including aromatic species and nitrogen- and oxygen-bearing molecules [1-3]. Combined with evidence for a moderately alkaline subsurface ocean in contact with a rocky core and ongoing hydrothermal activity [4-6], these findings indicate that Enceladus hosts an active internal geochemical environment relevant to habitability. However, whether the detected organics formed endogenously or derive from primordial material remains uncertain [1-3].

Here we present laboratory simulations of organic synthesis under hydrothermal (≤ 150 °C) and freezing (down to -40 °C) conditions using starting solutions representative of Enceladus' ocean and cometary building materials, including HCN, NH_3, aldehydes, and dissolved inorganic carbon [6-8]. Heating-only, freezing-only, and cyclic heating–freezing experiments were conducted to mimic molecular exchange between Enceladus' rocky core, ocean, and ice shell [9]. Reaction products were analyzed by HPLC, NMR, UV-vis spectroscopy, and Laser-Induced Liquid Beam Ion Desorption Mass Spectrometry (LILBID-MS), enabling direct comparison with Cassini Cosmic Dust Analyzer (CDA) data [10].

Our experiments show that hydrothermal reactions efficiently generate a wide range of N- and O-bearing organics, including amino acids (e.g., glycine, alanine, serine, and aspartate), amines, aldehydes, nitriles, and carboxylic acids, likely primarily through aldehyde-cyanide-ammonia chemistry analogous to Strecker-type synthesis [11]. Freezing alone also assists in producing simple amino acids such as glycine, consistent with concentration-driven reactions in brine pockets within ice [12]. The molecular signatures of our products match many of the low-mass organic compounds detected in Enceladus' plume [2, 3], supporting a deep, hydrothermal source for a substantial fraction of the observed organics. In contrast, aromatic-rich macromolecules and long unsaturated hydrocarbon chains reported in plume particles [1] were not reproduced, implying additional contributions from primordial organic matter or higher-temperature catalytic processes.

By coupling models of Enceladus' interior (ocean chemistry, ice-shell exchange, and thermal cycling) with laboratory chemistry and flight-analogous mass spectrometry, this study illustrates how internal planetary processes are expressed as measurable molecular signatures. Our results demonstrate that organic compounds and their detectability are strongly controlled by environmental context: temperature conditions govern molecular diversity, whereas freezing and salinity may influence partitioning and instrumental response, respectively. Direct simulation of Cassini CDA measurements using LILBID-MS provides a quantitative link between laboratory products and spacecraft observations. Together, this interdisciplinary approach links planetary interior processes, laboratory experimentation, and mission data, offering a transferable framework for interpreting organic detections and assessing habitability across diverse planetary environments explored by past, present, and future missions.

References: [1] Postberg F. et al. (2018) Nature, 558, 564-568 [2] Khawaja N. et al. (2019) Mon. Not. R. Astron. Soc., 489, 5231-5243. [3] Khawaja N. et al. (2025) Nat. Astron., 9, 1662-1671. [4] Choblet G. et al. (2017) Nat. Astron., 1, 841-847. [5] Sekine Y. et al. (2015) Nat. Commun., 6, 8604 [6] Waite J. H. et al. (2017) Science, 1979, 155-159. [7] Peter J. S. et al. (2023) Nat. Astron., 8, 164-173. [8] Waite J. H. et al. (2009) Nature, 460, 487-490. [9] Soderlund K. M. (2020) Space Sci. Rev., 216, 80. [10] Klenner F. et al. (2019) Rapid Commun. Mass Spectrom., 33, 1751–1760. [11] Miller S. L. and Van Trump J. E. (1981) In: Wolman, Y. (eds) Origin of Life. Springer, Dordrecht. [12] Miyakawa S. et al. (2002) In: Orig Life Evol Biosph, pp. 209–218.

Deciphering the evolution of aqueous environment on Mars: Geomorphological perspectives

Hitoshi Hasegawa[1]

[1]Faculty of Science and Technology, Kochi University
(Akebono-cho 2-5-1, Kochi 780-8520, Japan: e-mail: hito_hase@kochi-u.ac.jp).

Mars is considered to have had a thick atmosphere and warm and humid environment conducive to extraterrestrial life around 3.8 billion years ago. Most of the early liquid water dissipated into space about 3.5 billion years ago, and the present-day Mars has only a thin atmosphere and extremely cold and dry environment. However, recent thermodynamical model suggested that salt brine may also exist in liquid form at high latitudes [1], and that it may be possible for extant organisms to exist in relation to the brine. Therefore, Mars is a unique extraterrestrial planet for which the persistence and evolution of habitable environments can be examined. In this presentation, we introduce our ongoing research attempting to decipher the aqueous environmental history of Mars, by focusing on (1) deltas and (2) desiccation polygon landforms.

In Topic (1), we examined the delta topography on the Martian surface and its formation mechanisms using the tank experiments at Nagasaki University. We identify two distinct delta types: "lobe-extruding deltas" formed during water-level falls and "stepped deltas" formed during rising water levels. The lobe-extruding deltas appear near proposed paleo-coastlines and date to ~3.8–3.2 Ga, consistent with a global ocean regression during the Hesperian. In contrast, stepped fan-deltas are found at a wider range of elevations and younger ages (~2.0–0.1 Ga), suggesting isolated, short-lived lakes that formed during the Amazonian. Our findings constrain the timing of planetary-scale transition from global hydrosphere to localized aqueous environments, and refine the understanding of Mars' paleoclimate evolution and potential habitability.

In Topic (2), we are attempting to verify the Martian aqueous environments during the Amazonian period. Some previous studies [2,3] reported that Crater Floor Polygons observed at 50°–70° latitudes on both hemispheres of Mars exhibit similarities to the desiccation-related polygonal terrains on Earth, suggesting a possibility of surface aquatic environment during the Amazonian period. In this study, we performed satellite and field investigations of two morphological types of desiccation polygons (so-called “Raised rim polygons” and “Low rim polygons”) in the southwestern USA and Atacama Desert, Chile, in conjunction with previous studies in China [4,5]. Applying these findings based on the terrestrial analog sites, we discuss Martian aquatic environments possibly developed during the Amazonian period.

References: [1] Rivera-Valentín E. G. *et al*. (2020) *Nature Astronomy*, 4, 756–761. [2] El-Maarry M. R. *et al*. (2010) *JGR: Planets*, 115, E10. [3] El-Maarry M. R. *et al*. (2014) *Icarus*, 241, 248–268. [4] Dang Y. *et al*. (2020) *JGR: Planets*, 125, e2020JE006647. [4] Mangold N. (2005) *Icarus*, 174, 336–359. [5] Cheng R. L. *et al*. (2021) *Geomorphology*, 383, 107695.

A comparative study of windward slope gradients of transverse dunes on Mars and Earth

Y. Kodama[1], S. Matsushima[2], M. Umehara, P.B. Hiral[3] and R. Trishit[3]

[1] Dept. Life and Environmental Agriculture Sciences, Faculty of Agriculture, Tottori University (kodamda@tottori-u.ac.jp), [2] Student, Faculty of Agriculture, Tottori University, [3] Institute for Planetary Materials, Institute for Planetary Materials, Okayama University.

I. Introduction

Under high availability of fine-sand conditions, transverse dunes are formed by unidirectional prevailing winds. Previous research has revealed that the inclination angle of the leeward slope of transverse dunes on Mars and Earth is approximately 32° [1]. Regarding the inclination angle of the windward slope of transverse dunes, very few studies have been conducted [2]. The purpose of this study is to compare the inclination angle of the windward slope of transverse dunes under the different planetary environments of Mars and Earth.

II. Research and Analysis Methods

A region where transverse sand dunes are clearly visible was selected as the study area [3]. For Mars, we selected the area centered at 147.98°W, 79.26°N near the North Pole. For Earth, we selected the area centered at 85.67°E, 40.05°N in the Taklamakan Desert. We imported DEM data from each study area into QGIS and created cross-sectional survey lines perpendicular to dune crest lines to obtain topographical profiles. Then the wavelength and relative height of the dunes were measured. Furthermore, we calculated the slope angles of the straight slope sections on the windward.

III. Results and Discussion

Earth's transverse dunes were approximately five times larger than those on Mars, demonstrating a significant difference between the two. Meanwhile, the ratio of relative height to wavelength was similar, ranging from 0.03 on Mars to 0.04 on Earth, indicating that the dune shape ratios were similar on both planets. The distribution of slope angles on the windward slopes reveals similarity between Mars and Earth (Fig.1). On Mars, the most common value was 7-8°, with the overall range concentrated between 5-12°. On Earth, the most common value was 7-8°, with a distribution range of 5-10°. This very similar distribution of slope angles on the windward slopes, despite the different planetary environments, suggests that the basic sand transport processes in dune formation may be common on both planets.

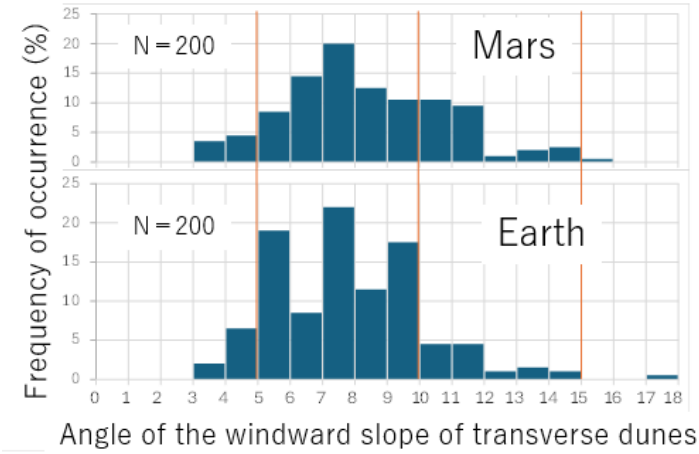

Fig.1 Comparison of the slope angles of the windward slopes of transverse dunes

IV. Conclusions

The slope angle of the windward slope of transverse dunes on both Mars and Earth showed a very similar distribution, with a modest value of 7-8°. Future work will require conducting similar analyses on Mars and Earth in low-latitude regions less susceptible to freezing, and examining the influence of environmental factors in more detail.

References: [1] Rubanenko et al. (2024) Mars Polar Science, 6069pdf [2] Umehara, M. (2011) Master's thesis, Graduate School of Regional Sciences, Tottori University, 45pp. [3] Chao, L, and Zhibao, D. (2022) Frontiers in Astronomy and Space Sciences, 9, Article 811702. 1-12.

Integrated Spectral Analysis and Web-GIS/VR System Development for Mars

Y. Ogawa[1], S. Yamaguchi[1], S. Kimura[1], A. Sakurai[1] and K. Okazaki[1], and M. Ohtake[2]

[1] The University of Aizu (Aizuwakamatsu City, Fukushima 965-8580, Japan, yoshiko@u-aizu.ac.jp), [2] Okayama University (Yamada 827, Misasa, Tottori 682-0193, Japan).

We have been working on three research topics related to Mars: (A) integrated spectral analysis to search for traces of water, (B) development of a Mars Web-GIS for visualizing VNIR spectral data, and (C) implementation of immersive virtual reality (VR) environments at rover observation sites to facilitate intuitive understanding of terrain features, with the aim of contributing to future rover mission planning and operations.

As for (A), we began by developing a new tool that enables integrated analysis of CRISM and SHARAD data [1]. CRISM data allow detection of absorption bands characteristic of hydrothermal minerals and clarification of their spatial distribution. SHARAD data enable identification of subsurface dielectric discontinuities, which may correspond to potential permafrost layers on Mars. We adopt the DBSCAN algorithm for clustering the discontinuities and then they are interpolated to construct a spatially continuous gridded layer by Kriging method. The locations where hydrous minerals were detected through CRISM data analysis are integrated into SHARAD 3D mapping results using geographic information. By combining analytical results from CRISM and SHARAD data, we can visualize and examine the correlation between their spatial distributions, obtaining insights into the ancient aqueous environments on Mars. The tool is currently being applied to datasets from rover exploration sites, including Gale Crater and Jezero Crater.

As for (B), we have developed and continuously extended the Mars Web-GIS "Red Ace" [e.g., 2]. Red Ace was originally designed to visualize CRISM and THEMIS spectral data overlaid on topographic layers through a web browser, enabling users to easily access and explore spectral datasets. The system has since evolved to incorporate analysis functions. The latest version implements fundamental VNIR spectral analysis functions, including similarity analysis. Users can directly compare observed CRISM spectra with laboratory spectral data from a spectral library, visualize the results within the browser interface, and download the data for further analysis. Dynamic map rendering and seamless zooming performance are supported through MapProxy and the Web Map Tile Service (WMTS) protocol.

Over the past two years, we have initiated project (C), the development of Mars VR environments. While conventional web-based 2D visualization tools (such as Red Ace described above), provide access to Martian datasets, they are often insufficient for intuitively perceiving terrain relief and interpreting observational data within their spatial context. Therefore, we aim to develop immersive VR environments at rover observation sites, specifically in Gale Crater and Jezero Crater, explored by the Curiosity and Perseverance rovers, respectively. The proposed system enables integrated 3D visualization of Martian terrain and associated observational data within a unified spatial framework. The environment is designed to balance locomotion efficiency with spatial cognition, allowing users to effectively explore large-scale terrain. The system incorporates textured terrain models and provides functionalities such as natural walking locomotion, navigation via an Overview Mode, instantaneous warping to arbitrary locations, and real-time display of latitude, longitude, and azimuth information.

We expect that our tools and the analytical results derived from them will enhance understanding of the Mars surface environment and support future Mars rover missions.

References: [1] Hidaka, M. and Y. Ogawa (2023) 54th Lunar and Planetary Sci. Conf. 2023, #2806. [2] Usui et al. (2023) AGU Fall mtg 2023, #IN51B-0413.

ESTIMATED LUNAR MANTLE COMPOSITION BY SLIM MULTIBAND CAMERA

M. Ohtake[1], K. Saiki[2], Y. Nakauchi[2], H. Nagaoka[2], R. Miyazaki[3], M. N. Nishino[3], S. Yamamoto[4], H. Sato[3], C. Honda[5], Y. Ishihara[3], R. Nishitani[3], I. Kajitani[3], and Y. Yokota[6]

[1] Okayama University (Yamada 827, Misasa, Tottori 682-0193, Japan, mohtake@okayama-u.ac.jp),[2]Ritsumeikan University (1-1-1 Noji-higashi, Kusatsu, Shiga525-8577, Japan), [3]Japan Aerospace Exploration Agency (7-44-1 Jindaiji Higashi-machi, Chofu-shi, Tokyo 182-8522, Japan), [4]National Institute of Advanced Industrial Science and Technology, Japan (1-1-1 Umezono, Tsukuba, Ibaraki 305-8561, Japan), [5]The University of Aizu (Ikki Machi, Tsuruga, Aizu Wakamatsu City 965-8580, Japan), [6]Institute of Science Tokyo (2 Chome-12-1 Ookayamaya, Megro, Tokyo, 152-8550, Japan)

Previous remote-sensing data obtained by the SELENE (Kaguya) Spectral Profiler (SP) found exposures with olivine-rich spectral features, globally distributed on the lunar surface [1]. These olivine-rich exposures possibly originated from the mantle that is excavated from depth by basin-forming impacts. However, as previous lunar sample analyses indicate that olivine-rich rocks on the Moon have three major origins: 1) mantle material, 2) olivine-rich volcanic material, and 3) olivine-bearing crustal intrusion (troctolite), we tried to estimate Mg# (Mg/(Mg+Fe) in mole per cent) for these olivine-rich spectra to assess origin of the previously identified olivine exposures by [1] and to estimate Mg# of the lunar mantle. And based on the results, we identified locations of likely olivine exposures originated from mantle in a global scale [2]. Among the identified olivine exposures likely mantle origin, we selected one location near the fresh crater Shioli (270 m in diameter), situated outside the southern rim of Theophilus (11.4◦ S, 26.4◦ E) as the landing site for Japanese lunar explorer, Smart Lander for Investigating Moon (SLIM) mission.

After the successful launch on September 7, 2023, the SLIM landed on the lunar surface on January 20. After the successful landing on the lunar surface, we obtained spectral images of the lunar surface rocks by Multiband Camera (MBC) data carried by the SLIM. The MBC has a telescopic optical system capable of near-infrared high-spatial-resolution observation in 10 bands. The band assignments are 750, 920, 950, 970, 1,000, 1,050, 1,100, 1,250, 1,550, and 1,650 nm, and its spatial resolution is 1.1 mm/pixel at 10 m for mineralogical-scale observation. At the lunar surface, the MBC started observation in a scanning mode to create mosaiced image of the landing site. Dark level correction, integration time correction, and conversion factors from raw signals (DN) to the input energy for the pixels in each band derived by prelaunch integrating sphere tests data were applied to the raw signals. Then, relative reflectance images were derived.

In this study, we investigated mineralogy and rock texture of one olivine bearing rock labeled as “Dalmatian” by using the MBC spectral images. The rock consists of two units; one unit is large olivine clasts (up to 3 - 4 cm in diameter) and the other is mixture of olivine and low-Ca pyroxene. The olivine clasts are surrounded by the olivine and low-Ca pyroxene unit, exhibiting a patchy, intricate texture. No plagioclase or high-Ca pyroxene grains are identified in the olivine clasts unit. The lack of plagioclase and the large size of the olivine clast in Dalmatian indicate that the origin of this unit is plutonic. Based on the observed rock texture, significantly mafic-rich mineralogy, Mg# consistent to the lunar mantle (Mg# was estimated by comparing absorption center wavelength of olivine obtained by the MBC to laboratory measurements of synthetic olivine with variable Mg#), and geologic setting (geological setting was analyzed by using the SELENE (Kaguya) Multiband Imager data), we interpret that the olivine clasts in Dalmatian originated from the mantle. Comparison of the estimated Mg# of olivine from global remote sensing data by the SP and the landing observation by MBC with previous simulation models of the lunar magma ocean solidification, starting with different lunar magma ocean composition, enable us to estimate chemical composition of the bulk lunar mantle.

References: [1] Yamamoto S. et al. (2010) Nature Geoscience, 3, 533-536. [2] Ohtake M. et al. (2024), *55th LPSC, abstract* #1927.

Compact Spacecraft Potential Sensor Using Charge-Induced Optical Absorption in a Silicon Photonic Waveguide

Yasushi Takahashi

Fuculty of Environmental, Life, Natural Science and Technology, Okayama University, 700-8530, Japan
y-takahashi@okayama-u.ac.jp

Electrostatic discharge (ESD) triggered by spacecraft charging remains a major reliability concern for satellites, especially in the rapidly growing low-Earth-orbit (LEO) sector. Charging arises from interactions with ambient plasma and energetic particles, producing a potential difference ΔV between the spacecraft (floating potential) and the surrounding plasma (plasma potential). When $|\Delta V|$ becomes large (e.g., $\Delta V < -100$ V), the probability of ESD events increases because different spacecraft surfaces can charge non-uniformly. However, ΔV fluctuations in orbit have been measured only in limited cases, and the lack of compact, robust sensors has constrained data acquisition and quantitative risk assessment.

Here we present a compact ΔV sensor (photonic charge sensor) that uses an optical rather than an electrical conduction mechanism, enabling high resistance to ESD and improved suitability for space environments [1]. The sensing principle is based on charge-induced free-carrier absorption (FCA) in a silicon waveguide [2]. When the spacecraft potential becomes negative relative to the surrounding plasma ($\Delta V < 0$ V), positive ions are accelerated toward exposed conductive parts and toward a silicon photonic chip mounted on a metal plate. Upon reaching the silicon surface, incident ions can be neutralized by electron transfer, generating holes in the top silicon waveguide layer. Because an insulating layer suppresses charge escape, the accumulated hole density in silicon increases until the silicon potential approaches the plasma potential (ΔVSi = 0 V). Under this scenario, the final hole density becomes proportional to ΔV, and the guided optical power decreases exponentially with FCA, allowing ΔV to be estimated from optical attenuation. Importantly, the method does not depend on measuring changes in electrical conduction and is therefore expected to be intrinsically tolerant to ESD events.

We realized this concept in a fiber-coupled module integrating a silicon photonic waveguide (length ~0.8 mm). Light is coupled into and out of the waveguide using integrated small lenses and optical fibers inside a compact housing. To emulate a space plasma environment, we conducted experiments in a ~1-meter-diameter vacuum chamber equipped with a Xe plasma emitter. In the demonstrated conditions, the plasma density was comparable to typical LEO values.

The measurements verified the proposed mechanism. As ΔV became more negative, the transmitted optical power decreased monotonically. Stepwise changes from 0 V to negative values produced immediate and reproducible transmission drops. For sufficiently large $|\Delta V|$, the attenuation followed a simple ΔV–absorption relation. The response covered the ESD-relevant range ($\Delta V < -100$ V) and remained measurable down to −250 V. Occasional spike-like transients at high negative bias, attributed to discharge events in the chamber, did not damage the module after repeated runs.

This photonic approach offers a pathway to miniaturized, low-power spacecraft potential monitoring. The total power requirement of the overall sensor system (light source, photodetectors, and signal processing) is estimated to be on the order of 0.1 W. Future work will focus on improving sensitivity and response dynamics through surface engineering (e.g., passivation to mitigate charge trapping), optimizing module geometry to enhance plasma–silicon interaction, and extending characterization to broader plasma species and temperature compensation relevant to on-orbit deployment.

References: [1] Otsuka K., et al. (2026) npj Nanophotonics, 3:10. [2] Fujimoto M., et al. (2023) Opt. Continuum, 2, 349.

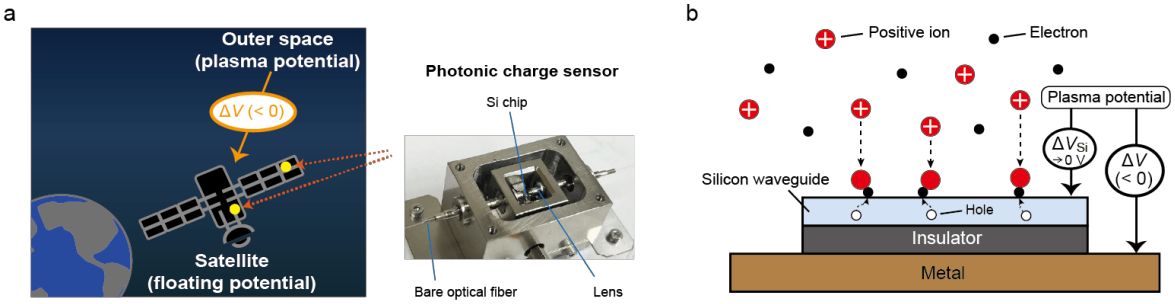

Fig. 1. **a** Illustration of the potential difference between a spacecraft and the surrounding plasma, ΔV and photograph of the photonic charge sensor module. **b** Principle of measuring ΔV using a silicon photonic waveguide.

Why Did Our Lunar Near-Infrared Spectral Cameras Take This Design?
— The Development History of Spaceborne Instruments with Potential Relevance to Mars Exploration —

Kazuto Saiki[1],

[1] Earth and Space Exploration Center, Ritsumeikan University, Kusatsu 525-0058, Japan, ksaiki@fc.ritsumei.ac.jp

I led the development of two near-infrared (NIR) spectral cameras for lunar missions. As planetary exploration increasingly emphasizes life-science objectives, a shared challenge across disciplines remains the same: translating scientific questions into space-qualified instruments. In this presentation, I summarize the development of these cameras and highlight practical lessons for future mission payload design.

My first involvement in planetary exploration was with the Lunar Imager & Spectrometer onboard the Japanese lunar orbiter Kaguya. At that time, I had no prior experience in near-infrared observations or remote sensing. My background was in meteoritics and experimental petrology, using scanning electron microscopy (SEM) with electron microprobe analysis, X-ray diffraction (XRD), and high-temperature furnaces for melting and crystallization experiments. To acquire first-hand knowledge of remote sensing, I initiated ground-based lunar observations using a commercial telescope equipped with band-pass filters and a monochrome CCD camera. With a total budget of approximately one million yen, I constructed my first visible-to-NIR spectral imaging system. Using this setup, I successfully reproduced FeO and TiO_2 distribution maps originally derived from Clementine mission data [1]. Although the hardware was simple, the calibration procedures and data-processing methods were fundamentally identical to those used in space missions. This experience provided critical practical understanding and became the foundation for subsequent funding and instrument development.

The next major project was the Advanced Lunar Imaging Spectrometer (ALIS), originally designed for deployment on the International Space Station (ISS). Its objective was to measure the Moon's spectral radiance with high precision, enabling its use as a radiometric calibration standard for Earth-observing satellites. The instrument featured a custom reflective telescope with dual optical paths for visible and near-infrared wavelengths and grisms for spectral dispersion. By scanning the lunar image with a mirror system, it was capable of acquiring three-dimensional spectral datasets (two spatial dimensions plus one spectral dimension) across 380–2400 nm. Although the instrument was successfully developed, the ISS payload opportunity was canceled before flight validation. Nevertheless, the project contributed significantly to fundamental lunar spectroscopy research.

Even during periods when Japanese lunar exploration concepts such as SELENE-B and SELENE-2 were proposed and subsequently discontinued, I continued refining spectrometer designs. Various approaches—including liquid crystal tunable filters and acousto-optic tunable filters (AOTF)—were evaluated. However, from the standpoint of structural simplicity, thermal and vibration robustness, and reliability in harsh space environments, band-pass filter systems and diffraction-grating spectrometers remained the most dependable solutions.

Following the revival of lunar exploration activities, I led the development of two flight instruments: the Multi-Band Camera (MBC) onboard the SLIM lunar lander and the Advanced Lunar Imaging Spectrometer (ALIS) for the LUPEX rover mission [2]. The former was designed for lithological identification and estimation of mantle-derived mineral chemistry, while the latter was optimized to detect as little as 0.5 wt% water ice in lunar polar regolith. Instrument architecture is governed not only by scientific objectives but also by operational constraints. The MBC employs a two-dimensional snapshot multi-band filter system to rapidly identify olivine-rich rocks within the limited operational lifetime of a lander. In contrast, the LUPEX ALIS adopts a line-by-wavelength diffraction-grating spectrometer configuration to detect weak 1.5 μm water-ice absorption features under restricted illumination conditions.

For researchers planning life-science exploration on Mars, a critical message emerges: defining a detection threshold—whether Mg# of olivine, wt% of water, or ppm-level organic abundance—is only the starting point. That threshold must be quantitatively translated into required signal-to-noise ratios (S/N), functional and optical design parameters, calibration strategies, environmental robustness, and operational timelines. An integrated systems-level design philosophy is indispensable. I conclude by synthesizing lessons learned through these development efforts and discussing practical strategies for designing observational instruments that reconcile scientific rigor with operational reality. I hope these experiences will contribute to future lunar and Martian exploration missions.

References: [1] Lucey P.G., Blewett D.T., and Jolliff B.L. (2000) *JGR*, 105, E8, 20297- 20305.
[2] Saiki K. et al. (2021) *Lunar Planet. Sci. Conf.* 52nd, 2548.

Development of VIS–NIR Multi-band and Hyperspectral Imaging Instruments for Lunar and Mars Landing Missions

Y. Nakauchi[1], H. Nagaoka[1], M. Ohtake[2], T. Morota[3], R. Fukunaga[1], A. Kakogawa[1]

[1]Ritsumeikan University (1-1-1 Noji-higashi, Kusatsu, Shiga525-8577, Japan; nakauchi@fc.ritsumei.ac.jp), [2]University of Aizu (Ikki Machi, Tsuruga, Aizu Wakamatsu City 965-8580, Japan), [3]The University of Tokyo (7-3-1 Hongo, Bunkyo-ku, Tokyo 113-0033, Japan.)

Introduction: The opportunities of landing exploration on the Moon and Mars are increasing. To advance the exploration and development of the Moon and Mars by leveraging these opportunities, high-performance yet lightweight scientific instruments capable of detailed in-situ analysis of regolith and boulders composition are indispensable. Direct on-site analysis of regolith and boulders enables flexible geological investigations and the selection of high-priority samples in the field for sample return, thereby significantly enhancing the scientific return of exploration missions. We have been developing several types of visible and near-infrared spectrometers for planetary exploration. Currently, we are focusing on the development of a multiband camera for wide-area observations, a microscopic hyperspectral camera, and a handheld spectroscopic analysis unit, all operating in the visible and near-infrared (400–1700 nm) wavelength range [1]. The reflectance spectra of lunar and Martian minerals exhibit characteristic absorption features in this wavelength range, allowing for the estimation of their composition.

Design of Microscopic Hyperspectral imager: One of the instruments currently under development is a compact VIS-NIR microscopic hyperspectral imager (Fig.1). It is composed of a SWIR camera (IMX 990, provided by Sony Corporation), auto focus lens, lens food, and VIS-IR light source. The sensor has sensitivity at wavelength from 400 to 1700 nm, which covers the characteristic absorption bands of lunar and Martian minerals and water ice. This sensor has 1296 (H) × 1032 (V) pixels with 5 μm pitch. The macro-optical system can focus on objects at working distances ranging from 50 to 70 mm. The field of view is 10 × 10 mm, corresponding to a spatial sampling of 10 μm/pixel at a working distance of 60 mm from the lens tip. The autofocus system has already been demonstrated on the lunar surface by the MBC onboard SLIM [2]. Spectral light is delivered to the sample surface via an optical fiber, whose tip is fixed to the lens hood. The spectral resolution of the light source can be selected as either 2 nm or 20 nm.

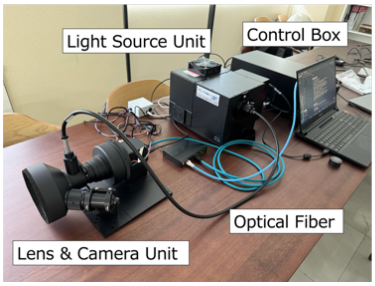

Fig.1) The laboratory model of microscopic hyperspectral

Experiment: The high spatial resolution image and continuous spectral data were obtained using developed laboratory model. The samples are lunar meteorite (mirror polishing), olivine (75 < d < 125 μm), epidote (unsaved), water ice (75 < d < 125 μm), methane gas. Mixed samples of olivine–epidote and olivine–water ice were prepared, with mixing ratios of 1:1 and 88.1:11.9 wt%, respectively. As an example, In Fig.2 shows the microscopic image and continuous reflectance spectra results of olivine–epidote mixture. Distinct absorption features corresponding to different minerals are clearly observed.

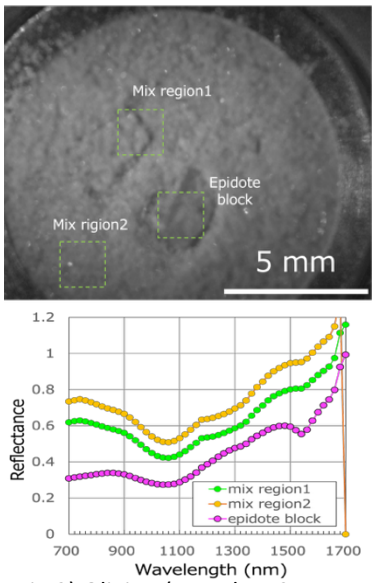

Fig.2) Olivine (75 < d < 125 μm) and epidote (unsaved) mixture sample. The laboratory model of microscopic hyperspectral

Imprecation and Summary: We are developing VIS–NIR multiband and hyperspectral imagers for lunar and Martian exploration missions. Our spectroscopic imaging system can simultaneously acquire high-spatial-resolution image data and continuous spectral data, enabling the detection of anhydrous and hydrous minerals, as well as volatile components. Experimental results demonstrate that the system is applicable to lunar and Martian exploration and to compositional analysis in laboratory environments.

Furthermore, we are currently developing a handheld analytical unit equipped with a hyperspectral camera. In this presentation, we will introduce an overview of the instruments under development and discuss their applicability to fieldwork.

References: [1] Y. Nakauchi et al., (2025) LPSC, abstract #2279. [2] Saiki, K. et al. (2024) 21th AOGS, ab-struct#PS16-A013.

FROM PRESERVATION TO SUBLIMATION: ICE STABILITY IN MARTIAN MID-LATITUDE CRATERS

H. Bijoy1, T. Ruj1, J. Kameda1, J. W. Head2, T. Sako1, G. Komatsu3,1Institute for Planetary Materials, Okayama University, Tottori 682-0193, Japan, 2Department of Earth, Environmental and Planetary Sciences, Brown University, Providence, Rhode Island 02912, USA, 3International Research School of Planetary Sciences, Università d'Annunzio, Viale Pindaro 42, 65127 Pescara, Italy. (hiralpb@s.okayama-u.ac.jp)

Near-surface water ice, occurring either as relatively pure deposits or intermixed with regolith, is widespread across the Martian mid-latitudes (30°–60° in both hemispheres) [1]. These ice-rich materials record episodes of volatile redistribution and provide key constraints on Amazonian climate variability. Impact craters represent well-defined geomorphic settings in which ice accumulation and preservation are modulated by crater-scale topography, particularly along interior depressions and pole-facing slopes. Many mid-latitude craters contain debris-mantled, ice-rich infill deposits, commonly termed ice-rich crater fills (IRCFs), that preserve evidence of repeated deposition and modification. However, previous studies have primarily emphasized ice volume estimates and present-day distribution [2,3], with less focus on linking crater-fill morphology to the regional processes governing ice stability and degradation.

To address this gap, we systematically mapped and classified more than 5,000 ice-rich crater fills (≥2 km in diameter) across the northern mid-latitudes (25°–60°N), interpreting these deposits as a continuum of preservation and degradation states rather than discrete morphologic categories. Spatial analysis of crater-fill types was used to evaluate the combined influence of climatic forcing and local geomorphic setting on ice accumulation, sublimation, and long-term stability within crater interiors. Mapping was conducted in ArcGIS Pro using Context Camera (CTX; ~6 m/pixel) imagery for regional coverage, supplemented by High-Resolution Imaging Science Experiment (HiRISE; ~0.3 m/pixel) data for targeted validation and Mars Orbiter Laser Altimeter (MOLA; ~200 m/pixel) topography for morphometric context.

Based on this framework, mid-latitude crater fills were grouped into four morphologic categories representing progressive stages of ice modification. Type 1 exhibits flow-like textures and wall-confined ridges consistent with debris-covered, well-insulated ice. Type 2 shows concentric ridges and ring-mold features indicative of buried ice beneath a protective mantle. Type 3 is characterized by pits, fractures, and brain terrain reflecting sublimation-driven degradation and viscous relaxation. Type 4 displays polygonal and scalloped terrains associated with shallow, climate-sensitive ground ice. Together, these categories define a continuum from well-preserved ice-rich fills to ice-depleted crater interiors.

Correspondingly, IRCF distributions show systematic latitudinal and regional variability across the northern mid-latitudes. Preserved fills (Type 1, ~30%) and concentric forms (Type 2, ~12%) are concentrated between 25°–45°N, particularly in Arabia Terra and Tempe Terra, indicating efficient ice accumulation and long-term insulation under favorable climatic conditions. In contrast, degraded fills (Type 3, ~28%) dominate between 30°–50°N within Deuteronilus and Protonilus Mensae, where fractured and pitted morphologies reflect sublimation-driven modification. Moreover, shallow ice-bearing morphologies (Type 4, ~30%) are widespread between 40°–60°N in Arcadia and Utopia Planitia, consistent with near-surface ground ice responding to present environmental conditions. The highest concentration of preserved ice-rich fills occurs between 30°–42°N, supporting a latitudinal transition from stable, debris-insulated ice to progressively degraded and climate-sensitive ground ice.

Furthermore, high-obliquity conditions enhance atmospheric water redistribution from the poles to the mid-latitudes, promoting ice accumulation within crater interiors were reduced insolation favors preservation [4]. Between ~30°–40°N, well-preserved Types 1–2 fills reflect efficient deposition followed by debris insulation that limited sublimation and supported long-term subsurface stability. Conversely, Type 3 fills within Deuteronilus and

Protonilus Mensae indicate a sublimation-dominated regime, were thinner mantles and complex topography enhanced ice loss and viscous relaxation. At higher latitudes, polygonal and scalloped terrains in Utopia Planitia define shallow, climate-sensitive ground ice responding to ongoing sublimation under present environmental conditions [5].

Overall, the observed morphologic transitions among ice-rich crater fills indicate that mid-latitude impact craters record obliquity-driven cycles of ice accumulation and loss. These patterns define latitudinal zones of ice stability and degradation and provide a geomorphic framework for understanding cryospheric evolution on Mars.

References: [1] Butcher F. E. (2022) Water ice at mid-latitudes on Mars, Cambridge University Press. [2] Levy J. S. et al. (2010) Icarus, 209, 390–404. [3] Dickson J. L. et al. (2010) Earth Planet. Sci. Lett., 294, 332–342. [4] Madeleine J.-B. et al. (2009) Icarus, 203, 390–405. [5] Head J. W. et al. (2003) Nature, 426, 797–802.

Effect of iron content on viscosity of ringwoodite and its implication for the rheology of the Martian mantle

Zhiyuan Chen[1], Daisuke Yamazaki[1]

[1] Institute for Planetary Materials, Okayama University

Viscosity of Martian mantle has been estimated to be 2-6×10^{22} Pa·s from glacial isostatic adjustment of Mars's north polar ice cap, which is 1-2 orders of magnitude higher than that of the Earth (e.g., Lau et al., 2016; Samuel et al., 2019; Broquet et al. 2025). The Martian mantle is mainly composed of olivine and wadsleyite/ringwoodite as well as the Earth' mantle and hence the viscosities of these minerals are key to understand the rheology of the Martian mantle. The previous study on olivine viscosity showed that Fo_{90}, which is representative of the Earth's mantle composition, is approximately one order of magnitude larger than that of Fo_{75}, which may be representative in the Martian's mantle. The lower viscosity of Mars can be explained by lower temperature in the Martian mantle estimated to be ~200 °C lower than that of the Earth (Samuel et al., 2022). On the other hand, viscosity of deeper portion of the Martian mantle is not constrained from mineral physics due to the lack of experimental data on the wadsleyite and/or ringwoodite. In this study, we conducted the deformation experiments on ringwoodite to investigate the effect of iron content on viscosity.

We prepared ringwoodite aggregates with Mg# 40 and 75 as starting materials for deformation at 19 GPa and 1200 °C. Then we deformed two ringwoodite samples simultaneously by D111-type high-pressure deformation apparatus at 17 GPa and 1200 °C with displacement rate of d-ram of 2 μm/min. The samples were arranged in series along the deformation axis to have the same stress in the cell assembly. After experiments, we estimated the strain rate during deformation from the change of sample lengths.

Deformation mechanism in the present study may be dominated by dislocation creep as well as previous olivine deformation (Zhao et al., 2009) from microstructural observation including the wavy grain boundaries and dynamic recrystallization during deformation. Strain rate of ringwoodite with Mg# 40 is only ~1.5 times larger than that with Mg# 75. This iron effect is much smaller than the effect on olivine (Zhao et al., 2009), indicating the more than one order of magnitude higher viscosity than that inferred from observations (Broquet et al. 2025). To understand the observed viscosity, we need to investigate the additional factors such as effects of water, microstructure, and deformation mechanism.

HABITABILITY AT HIGH MARTIAN LATITUDES EXPLORED BY REMOTE SENSING, FIELD SURVEYS AND EXPERIMENTS

Takumu Chijiiwa[1], Hitoshi Hasegawa[2], Trishit RUJ[1], Izawa Matthew[1], Ohtake Makiko[1], Shohei Aoki[3], Goro Komatsu[4], Hiroki Shozaki[5], Sakiko Kikuchi[6], Anju Sakuma[7], Usui Tomohiro[8]

[1] IPM, Okayama Univ., Yamada 827, Misasa, 682-0193, Japan (takutaku1984@s.okayama-u.ac.jp), [2] Kochi Univ., Akebono-cho 2-5-1, Kochi, 780-8520, Japan, [3] Graduate School of Frontier Sciences, Tokyo Univ., [4] Universiá d'Annunzio, [5] ELSI, Institute of Science Tokyo, [6] JAMSTEC, [7] Tokyo Univ., [8] JAXA

Understanding the mineral composition of Martian sulfate deposits is essential for reconstructing past aqueous environments and assessing the current habitability of Mars. Spectroscopic observations have detected gypsum ($CaSO_4 \cdot 2H_2O$), a hydrous calcium sulfate, in the dune fields around Olympia Planitia [1]. Previous studies have suggested that liquid brines may exist transiently under current Martian environmental conditions, particularly at high latitudes, suggesting the possibility of liquid brines [2]. Additionally, Dark Dune Spots (DDS) found in this region show significant seasonal variations, which may be related to subsurface or near-surface brine processes [3]. However, observations at high latitudes on Mars are difficult due to noise, and it is unclear what minerals precipitate in the DDS. In this study, by combining field surveys and laboratory spectroscopic experiments, we clarified the mineralogical characteristics of the DDS and the formation process of gypsum dunes in more detail.

A field investigation was conducted at White Sands, New Mexico, USA, a terrestrial analog for Martian gypsum dunes due to its similar geomorphological setting and evaporite-driven sedimentary processes. At White Sands, evaporite minerals precipitate from Lake Lucero during the dry season and may contribute to the formation of gypsum dunes. X-ray diffraction (XRD) analyses of samples collected along a transect from Lake Lucero to adjacent dunes revealed clear spatial variations in sulfate mineral assemblages. Gypsum dominates dune sediments, whereas more soluble sulfate phases, including bassanite ($CaSO_4 \cdot 0.5H_2O$) and Na–Mg sulfates, are preferentially detected near the lake margin. The occurrence of bassanite, a metastable phase with higher solubility than gypsum, suggests precipitation under advanced evaporation and concentration conditions within the salt lake.

Furthermore, shortwave infrared (SWIR) reflectance spectroscopy demonstrated that the White Sands and mixed sulfate samples exhibited characteristic absorption features in the 1.92–1.96 μm wavelength range, demonstrating overlapping contributions from gypsum, bassanite, and highly soluble sulfates.This wide range of absorption signatures likely results from mineral mixtures associated with brine generation and evaporation processes. Thus, this absorption signatures provides a potential mineralogical signature for identifying past or present brine activity.

However, the data was noisy and lacked absorption at 1.5 μm, as seen in the mixed sample and White Sands, so it does not provide strong evidence. In the future, we plan to use a chamber that can reproduce the Martian environment to observe how the spectra and mineral phases of the White Sands and mixed sample change under the Martian environment, and apply this to Mars remote sensing.

Reference: [1] Langevin, Y., Poulet, F., Bibring, J. P., & Gondet, B. (2005). Science, 307(5715), 1584-1586. [2] Rivera-Valentín, E. G., Chevrier, V. F., Soto, A., & Martínez, G. (2020). Nature astronomy, 4(8), 756-761. [3] Kereszturi, A., Möhlmann, D., Berczi, S., Horvath, A., Sik, A., & Szathmary, E. (2011). Planetary and Space Science, 59(13), 1413-1427.

The Effect of Water on Martian Magma Ocean Evolution: Experimental Insights into dense silicate layer at the CMB

D.H.F. Diyalanthonige[1*] and T. Yoshino[1],

[1] Institute for Planetary Materials, Okayama University, Misasa, 827 Yamada, Misasa, Tottori 682- 0193, Japan
dilan_fernando@s.okayama-u.ac.jp

Seismic data from the Insight mission has altered our understanding of the Martian interior [1,2]. The interpretation of these data indicates the core surrounded by a stratified silicate molten layer referred to as the basal magma layer (BML) as a result of crystallisation of the early Martian magma ocean (MMO) [1,2]. The requirements for BML to exist are that it be a dense melt rich in iron and heat-producing elements, with a low melting point that avoid entrainment in MMO convection [1,2] at deep mantle conditions. However, the formation of the BML with the current proposed composition for the bulk silicate Martian mantle struggles to generate and survive throughout Mars' interior thermal history [1,2,3,4,5]. One potential mechanism by which dense silicates could remain molten at BML conditions is the presence of volatiles particularly water, whose presence of water has been confirmed on the surface and interior by various Mars remote sensing mission, meteorites and experimental models [6].

In this study, based on melting relations for the Martian mantle containing 2 wt.% H_2O at pressures of 5, 10, 15 and 20 GPa and temperature of 1000-2000°C, we consider the formation of an iron-rich hydrous melts that could have subducted to the core-mantle boundary during differentiation of the early MMO and form a primitive BML. The experiments were conducted using a Kawai-type multi-anvil apparatus and the assembly consist of a double capsule outer Pt and inner Re to avoid water to escape and keep the sample under a QFM buffer relevant for the Martian interior [3,4,5,6]. The densities of the melts were calculated using the partial melt composition and compared with the solid phase above the solidus through the thermodynamic model BurnMan [7].

Our results show that the presence of H_2O reduces the solidus and liquidus temperatures relevant to present Martian geotherm [1,2,4,6], allowing melts to exist at lower temperatures. At 5 to 15 GPa, the hydrous melts are insufficiently dense to sink relative to the surrounding solid phases. As temperature from liquidus decreases and melt fraction decreases, the iron concentration and density of the melts increase. At 5 and 10 GPa, the melts are not high enough to sink the solid phases. At 15 GPa melts density are higher than the surrounding solid phases but not dense enough to be able to reach the BML. The experiments at pressure below 20 GPa have shown that the melts are mostly denser, with high Fe concentration just above the solidus. At pressure conditions relevant to the BML (~20 GPa), the forming melts have been dense enough to sink through the solid phases lay on top of the core-mantle boundary. The calculated melt density in this region exceeds 4.0 g/cm³, predicted from the data from Insight [1,2] consistent with the combination of ringwoodite and majorite as solid phases. Just below the liquidus temperature at 20 GPa, as the melt fraction decreases, the density of the melts start to increases until the formation of ferropericlase at 2000°C, where the FeO concentration in the melt is the highest. At lower temperatures, the FeO concentration in the melt decreases, as progressive crystallisation of ferropericlase, ringwoodite and majorite preferentially partitions FeO into the solid phases, causing the density of the melt to decrease until reaching buoyancy.

The presence of water in the early Martian mantle can produce a hydrous and dense BML in the early stages of the MMO. The presence of ferropericlase may indicate that the BML might be stratified with different degrees of crystallisation like indicated in the recent literature [1,2]. The melt formed at 20 GPa, at 2000°C could produces at depths between 60 - 100 km above the CMB.

References: [1] Samuel, H., Drilleau, M., Rivoldini, A. *et al. Nature* **622**, 712–717 (2023). [2] Khan, A., Huang, D., Durán, C. *et al. Nature* **622**, 718–723 (2023). [3] Bertka, C. M. and Fei, Y. (1997). Journal of Geophysical Research Atmospheres, 102(B3), 5251-5264. [4] Duncan, M.S., Schmerr, N.C., Bertka, C.M., Fei, Y. (2018) Geophysical Research Letters 45, 10211-10220. [5] Dreibus, G., Wänke, H., 1987. Icarus 71, 225–240. [6] Dong, J., Fischer, R. A., Stixrude, L. P., & Lithgow-Bertelloni, C. R. (2021). AGU Advances, 2(1), e2020AV000323. [7] Cottaar S., Heister, T., Rose, I., and Unterborn, C. (2014). Geochemistry, Geophysics, and Geosystems, 15(4), 1164-1179

TERRAIN CLASSIFICATION ON SATURN'S MOON TITAN BY MACHINE LEARNING (PRELIMINARY RESULT)

K. Goromaru[1], H. Hasegawa[1]

[1] Faculty of Science and Technology, Kochi University, Kochi, Japan.

Saturn's largest moon Titan is recognized as the only Solar System body besides Earth that exhibits stable surface liquid cycling at present. Through 13 years of observation, Cassini's Synthetic Aperture Radar (SAR) and Visible and Infrared Mapping Spectrometer (VIMS) have played a key role in global mapping of Titan's terrain distribution [1]. However, existing research faces challenges in quantitatively classifying the complex terrain structures observed on Titan's surface and understanding their formation mechanisms. Here, we attempted to classify and map Titan's surface terrains using machine-learning. Specifically, an unsupervised learning approach was adopted to achieve objective and quantitative classification [2].

The SAR mosaic [3] was subdivided into meshes of 128 × 128 pixels (corresponding to approximately 1° × 1°), and each mesh was treated as an independent analysis unit. For each mesh, feature learning was performed using an auto-encoder. The resulting latent feature representations were then clustered using Gaussian mixture modelling. Each resulting cluster was subsequently compared with the six geomorphological units defined by Lopes et al. [1], and the unit most consistent with each cluster was identified through visual inspection. The meshes were then colored according to the corresponding geomorphologic unit and we adapted this workflow to two locations: Xanadu and Selk crater.

The geomorphologic map produced in this study was compared with that of Lopes et al. [1]. In the Xanadu and Selk crater regions, the clustering results are broadly consistent with Lopes et al. [1] and primarily composed of three major geomorphologic units—Dunes, Hummocky, and Plains—while Labyrinth, Craters, and Lakes are integrated into other units rather than being extracted as independent clusters. The differences with previous studies [1] are observed in some regions, which are likely caused by the use of different datasets. Lopes et al. (2019) classified geomorphologic units using not only SAR data but also Emissivity, Altimetry, and VIMS, integrating correlations among multiple datasets. Hence, we are now trying to integrate both SAR and VIMS data using four-dimensional images as input data.

References: [1] Lopes, R. M. C., *et al*. (2019) *Nature Astronomy*, 4, 228-233. [2] Gao, A. F., *et al*. (2021) *Proceedings of the IEEE/CVF conference*, 4294-4303. [3] Cassini RADAR Science Team. (2019) *Cornell University Library's eCommons Digital Repository.* https://doi.org/10.7298/knpx-8a85

Development of an analytical strategy to determine the compound and position-specific isotope values of non-derivatised extraterrestrial amino acids

Maya Hamaguchi[1], Christian Potiszil[1], Ryoji Tanaka[1]

[1] Institute for Planetary Materials, Okayama University

Carbonaceous chondrites contain both soluble organic matter (SOM), including biologically relevant compounds such as amino acids, sugars, nucleobases, and fatty acids, and insoluble organic matter (IOM), which consists of macromolecular materials with complex structures composed of aromatic and aliphatic carbon frameworks. SOM is directly important for understanding the evolution of prebiotic molecules, and among them, amino acids have been one of the most intensively studied molecular classes owing to their relatively high abundances and structural diversity in chondrites. Various formation pathways for amino acids have been proposed, including Strecker synthesis, Michael addition, and formose-type reactions. In particular, recent studies have suggested that the molecular diversity and isotopic characteristics of organic compounds in meteorites are highly consistent with formose-type reaction networks. Laboratory experiments have demonstrated that, through aldose condensation reactions, aldehydes and sugars can produce amino acids and nucleobases, while simultaneously generating or promoting the growth of IOM. However, it remains unclear which formation pathways were dominant for individual meteorites, and unidentified processes may also have contributed. Given the existence of such reaction networks linking multiple organic compounds, comprehensive analyses of diverse molecular species are essential for understanding the origin and evolution of prebiotic organic matter. Moreover, the combination of comparative analyses among natural meteorite samples and experimental verification of formation environments and reaction pathways represents a fundamental approach for constraining the conditions and mechanisms responsible for the synthesis of prebiotic organic molecules.

Over the past several decades, advances in isotope analytical techniques have enabled extensive discussions based on compound-specific isotope analysis (CSIA) of carbon, nitrogen, and hydrogen in meteoritic organic molecules. For amino acids, carboxylic acids, aldehydes, and ketones reported to date, gas chromatography–isotope ratio mass spectrometry (GC-IRMS) has been the dominant method owing to its high chromatographic resolution. In contrast, the HPLC-ESI-Orbitrap-MS system is expected to allow high-precision quantification and isotope analysis without derivatization, owing to the use of electrospray ionization (ESI). In addition to CSIA, position-specific isotope analysis (PSIA) of amino acids has advanced significantly in recent years, attracting attention as a powerful tool for directly testing hypothetical abiotic synthetic pathways by resolving intramolecular isotope distributions (Chimiak et al., 2021[1]; Zeichner et al., 2023[2]). These previous PSIA studies of meteoritic amino acids GC-Orbitrap-MS with derivatization.

In this presentation, we focused on glycine and β-alanine, which are abundant in meteorites and widely used as indicators of aqueous alteration. We synthesized these amino acid standards with three distinct carbon and nitrogen isotopic compositions and compared their isotopic values using ESI-Orbitrap-MS with those measured by EA-IRMS. Furthermore, it is required to develop the derivatization strategies for the measurement of PSIA of these amino acids by ESI-Orbitrap-MS to PSIA of meteoritic amino acids, and we will present the current progress of this method development. Furthermore, to more comprehensively constrain the formation pathways of meteoritic organic molecules, we are developing HPLC-ESI-Orbitrap-MS–based CSIA and PSIA methods applicable to a wide range of compounds beyond amino acids, such as aldehydes and ketones, which can be precursors of amino acids.

References:

[1] L. Chimiak, J.E. Elsila, B. Dallas, J.P. Dworkin, J.C. Aponte, A.L. Sessions, J.M. Eiler, Carbon isotope evidence for the substrates and mechanisms of prebiotic synthesis in the early solar system, Geochimica et Cosmochimica Acta, Volume 292, 2021, Pages 188-202, ISSN 0016-7037, https://doi.org/10.1016/j.gca.2020.09.026.

[2] Sarah S. Zeichner, Laura Chimiak, Jamie E. Elsila, Alex L. Sessions, Jason P. Dworkin, José C. Aponte, John M. Eiler, Position-specific carbon isotopes of Murchison amino acids elucidate extraterrestrial abiotic organic synthesis networks, Geochimica et Cosmochimica Acta, Volume 355, 2023, Pages 210-221, ISSN 0016-7037, https://doi.org/10.1016/j.gca.2023.06.010.

P-V-T equation of state of calcium ferrite-type $CaAl_2O_4$ up to 25 GPa and 1500 K by using a multi-anvil press and in-situ synchrotron X-ray diffraction

Jinze He[1], Elena-Marie Rogmann[1,2], and Takayuki Ishii[1]

[1] Institute for Planetary Materials, Okayama University, Misasa, Tottori, Japan
[2] School of Earth Sciences, University of Bristol, Bristol, BS8 1RJ, UK

$CaAl_2O_4$ exhibits multiple crystal structures depending on pressure and temperature. By multi-anvil experiments, multiple high-pressure phases of $CaAl_2O_4$ were determined. Under ambient conditions, the monoclinic phase (CA-I), which adopts a tridymite-type structure with space group P21/n, is stable[1]. At pressures of 1–2 GPa, CA-I transforms into the CA-II phase, which crystallizes in the m-$CaGa_2O_4$ structural type. At 3–4 GPa and temperatures of 900–1100 °C, two additional polymorphs, CA-III and CA-IV, have been obtained. The structure of CA-III has been not identified reliably; however, the orthorhombic symmetry is assumed for it. The CA-IV phase is stable above 980 °C[1-2]. At approximately 8 GPa, both CA-III and CA-IV transform into a $CaFe_2O_4$-type (CF-type) structure with space group Pnma[2]. Recent theoretical studies indicate that the stability field of CF-type $CaAl_2O_4$ nearly covers the entire P–T range of the Earth's mantle[3]. However, studies on the thermoelastic properties of CF-type $CaAl_2O_4$ at high pressure and temperature are currently lacking.

In this study, we conducted in situ X-ray diffraction measurements for CF-type $CaAl_2O_4$ using multi-anvil press at pressures up to about 25 GPa and temperatures to 1500 K. The lattice parameters of CF-type $CaAl_2O_4$ were determined and its equation of state was established. Derived P-V-T data were fitted to high-temperature Birch–Murnaghan equation of state (EOS). Derived thermoelastic parameters are isothermal bulk modulus K_{T0} = 190(4) GPa, pressure derivative of bulk modulus $K' = 5.1(5)$, with assumed temperature derivative of bulk modulus $(\partial K_0/\partial T)_P = -0.030(6)$ GPa/K, and volumic thermal expansivity with $\alpha_0 = a_0 + b_0 T$ with values of $a_0 = 2.35(22) \times 10^{-5}$ K^{-1} and $b_0 = 1.71(30) \times 10^{-8}$ K^{-2}. Based on these data, we discuss the elasticity and velocity properties of the CF-type $CaAl_2O_4$.

References:
[1] S. Ito, K. Suzuki, M. Inagaki, S. Naka. Materials Research Bulletin. 1980;15(1):925-932.
[2] Akaogi M, Hamada Y, Suzuki T, Kobayashi M, Okada M. Phys Earth Planet Inter. 1999;115(1):67–77.
[3] Eremin, N.N., Grechanovsky, A.E. & Marchenko. Crystallogr. Rep. 2016;61:432–442.

Sound velocity measurements of iron alloys by inelastic x-ray scattering and the implications for planetary interiors

D. Ikuta[1], E. Ohtani[2], H. Fukui[3,4], T. Sakamaki[2], D. Ishikawa[3,4], and A. Q. R. Baron[3,4]

[1] Institute for Planetary Materials, Okayama University, Misasa, Japan, [2] Department of Earth Science, Tohoku University, Sendai, Japan, [3] Materials Dynamics Laboratory, RIKEN SPring-8 Center, Sayo, Japan, [4] Japan Synchrotron Radiation Research Institute, Sayo, Japan.

The cores of the Earth and other terrestrial planets are thought to consist mainly of iron alloys with some other elements. The composition of the Earth's core has been studied by comparing the seismological model, Preliminary Reference Earth Model (PREM) [1], which provides density and sound velocity profiles corresponding to depth, with compression and sound velocity measurements from laboratory experiments. Despite these efforts, the types and amounts of light elements in the Earth's core are still debated. Therefore, accurately measuring the equation of state and sound velocity of iron and iron-light element alloys under high-pressure and high-temperature conditions are important. Recently, the InSight mission's seismic observations of Mars have begun to yield results [2,3,4], making such experiments increasingly significant. Many high-pressure and high-temperature compression experiments have been conducted under core conditions using a diamond anvil cell with synchrotron radiation sources [5]. On the other hand, high-pressure and high-temperature sound velocity measurements under these conditions have not been well studied due to technical difficulties [6,7].
To address the issue of lack of sufficient sound velocity data on iron alloys under high-pressure and high-temperature conditions, we have been working to improve the inelastic x-ray scattering (IXS) method for measuring sound velocity in metals under these conditions. At the BL43LXU beamline of SPring-8, which has a spectrometer with millielectron volt (meV) resolution for investigating phonon modes, we developed a newly designed Soller screen system to optimize the sound velocity measurements under high-pressure and high-temperature conditions. This system reduces background noise and obtains weak IXS signals diffracted from small and thin samples under core pressures [8]. We also improved the design of the diamond anvil to keep stable pressure during long IXS measurements [6]. These improvements allowed us to successfully measure the sound velocity of pure iron and metals at pressures exceeding 300 GPa, corresponding to the pressure of the Earth's inner core. To generate high temperatures, we developed a portable laser heating system (COMPAT) for measuring sound velocity at temperatures exceeding 2500 K [9]. Using these improvements, we conducted sound velocity measurements of iron-nickel and iron-light element alloys under high pressure and temperature conditions. We present our recent progress in IXS sound velocity measurements under the core conditions.

References: [1] Dziewonski A. M. and Anderson D. L. (1981) *Phys. Earth Planet. Inter.* **25**, 297-356. [2] Khan A. et al. (2023) *Nature* **622**, 718-723. [3] Samuel H. et al. (2023) *Nature* **622**, 712-717. [4] Bi et al. (2025) *Nature* **645**, 67-72. [5] Ikuta D. et al. (2021) *Commun. Earth Environ.* **2**, 225. [6] Ikuta D. et al. (2022) *Nat. Commun.* **13**, 7211. [7] Ikuta D. et al. (2023) *Sci. Adv.* **9**, eadh8706. [8] Baron A. Q. R. et al. (2019) *AIP Conf. Proc.* **2054**, 020002. [9] Fukui H. et al. (2013) *Rev. Sci. Instrum.* **84**, 113902.

Sound velocities of Fe-bearing ringwoodite and majorite garnet: Implications for Martian mantle seismic profiles

T. Ishii[1], L. Luo[2], J. F. Lin[2], Y.J. Ryu[3], D. Zhang[3], S. Chariton[3], V. B. Parakapenka[3]

[1]Institute for Planetary Materials, Okayama University, Misasa, 682-0193, Tottori, Japan (takayuki.ishii@okayama-u.ac.jp), [2] The University of Texas at Austin, Austin,TX, USA, [3] GeoSoilEnviroCARS, University ofChicago, Argonne, IL, USA.

Ringwoodite and majorite are the dominant high-pressure silicates expected in the Martian mantle at depths corresponding to ~15–23 GPa [1]. Their elastic properties strongly influence interpretations of seismic observations from the InSight mission [2,3], yet the effects of FeO on their sound velocities remain insufficiently constrained. Because Mars is more Fe-rich than Earth [4,5], experimentally determining the elastic behavior of Fe-rich mantle minerals is essential for constructing realistic Martian mantle models.

In this study, we synthesized Fe-rich ringwoodite with a composition of $(Mg_{0.66}Fe_{0.34})_2SiO_4$ and majorite garnet with a composition of $Mg_{0.75}Fe_{0.10}Al_{0.26}Ca_{0.07}Si_{0.84}O_3$ at 18-20 GPa and 1700-2300 K using a multi-anvil press. We successfully synthesized large single crystals with more than 100 µm. Synthetic samples with controlled FeO contents were characterized by Xray diffraction, electron microprobe analysis, and Fourie Transform Infrared spectroscopy prior to elasticity measurements. The compressional (Vp) and shear (Vs) wave velocities of these ringwoodite and majorite single crystals were measured by Brillouin light scattering (BLS) in externally heated diamond anvil cells (EHDACs) at pressures up to 25 GPa and temperatures up to 700 K.

The elasticity data obtained can provide constraints directly relevant to the thermal structure of the Martian mantle.

The FeO effect on adiabatic bulk modulus of ringwoodite was limited whereas its shear modulus has a negative FeO dependence. On the other hand, elastic properties of majorite were almost no compositional dependence. Both Vp and Vs of ringwoodite and majorite decrease systematically with temperature. Thermoelastic modeling of our results and literature data along a representative areotherm showed that *Vp* and *Vs* of FeO-bearing ringwoodite are approximately 7.5% and 11.0% higher than that of the majorite. Our results reveal that velocity profiles of these Martian deep-mantle minerals are more sensitive to variations in the ringwoodite/majorite (Mg/Si) ratio than to thermal and FeO chemical perturbations. The derived elastic moduli and velocity–density relationships were incorporated into forward models of Martian mantle seismic profiles.

By integrating our new elastic data with existing models of Martian mantle mineralogy and thermal structures, we calculated velocity profiles for different compositional scenarios. The best-fit model, when compared with available InSight seismic observations, suggests the Martian mantle contains approximately 67 vol.% ringwoodite and 33 vol.% majorite, suggesting a ringwoodite-rich aggregate in the Martian lowermost solid mantle. This composition, characterized by relatively reduced thermal conductivity, lower solidus temperature and enhanced capacity in carrying incompatible elements. The FeO-rich ringwoodite layer co-evolved with the molten FeO-rich silicate layer above the core-mantle boundary that was also reported in recent InSight observations [6].

References:

[1] Bertka, C. M., & Fei, Y. (1997) *J. Geophys. Res.: Solid Earth*, 102, 5251–5264.
[2] Banerdt, W. B. et al. (2020) Nat. Geosci. 13, 183–189.
[3] Lognonné, P. et al. (2020) Nat. Geosci. 13, 213–220.
[4] Dreibus, G., & Wanke, H. (1985). *Meteoritics*, 20, 367–381.
[5] Yoshizaki, T., & McDonough, W. F. (2020) *Geochim. Cosmochim. Acta* 273–162.
[6] Khan, A. et al. (2021) *Science*, 373, 434–438.

Experimental Investigation of Martian Mantle Mineral Phase Transitions under High Pressure and High Temperature Conditions

Dongliang Jiang[a,b], Takashi Yoshino[b*]

[a]Research Center for Earth and Planet Material Sciences, School of Earth Sciences, Zhejiang University, Hangzhou 310058, China
[b]Institute for Planetary Materials, Okayama University, Tottori 682-0193, Japan

Abstract:

The internal structure of Mars remains not well understood, and recent seismic evidence suggests potential mantle heterogeneity[1]. High-pressure and high-temperature experiments are crucial for testing competing thermal-compositional models and for interpreting planetary geophysical observations. We conducted experiments at 6~19 GPa using molybdenum capsules to simulate Martian mantle conditions. Two distinct starting compositions were investigated[2,3]: one based on the recent meteorite-derived model of Yoshizaki & McDonough (2020), and the other corresponding to the widely-used geochemical model of Wanke & Dreibus (1994). Both compositions were equilibrated under IW-buffered conditions to replicate Martian oxygen fugacity. Two geotherms were applied: a Homogeneous Mantle geotherm consistent with conventional layered interior models, and a Heterogeneous Mantle geotherm which includes a hot basal molten silicate layer (BML). The resulting phase assemblages may provide key mineralogical constraints for interpreting seismic velocity profiles and for refining models of the Martian interior.

References

1. Samuel, H., Drilleau, M. Rivoldini, A. et al. Geophysical evidence for an enriched molten silicate layer above Mars's core. *Nature* **662**, 712-717 (2023).
2. Yoshizaki, T. & McDonough, W. F. The composition of Mars. *Geochim Cosmochimi Acta* **273**, 137–162 (2020).
3. Wänke, H. & Dreibus, G. Chemistry and accretion history of Mars. *Philos Trans A Math Phys Eng Sci* **349 (1690)**, 285–293 (1994).

A first look at the reflectance spectrum of ringwoodite: Opening a new window to shock metamorphism and deep mantle processes on extraterrestrial bodies.

M. R. M. Izawa[1], T. Yoshino[1], M. Ohtake[1]
1. Institute for Planetary Materials, Okayama University 827 Yamada, Misasa, Tottori 682-0193, Japan (matthew_izawa@okayama-u.ac.jp)

Hypervelocity shock is a process which has affected every solid surface in the solar system. During shock compression, rock-forming silicate minerals may be converted to polymorphs which remain metastable at ambient conditions after shockwave passage. Such shock-generated phases have been documented in terrestrial, martian, lunar, and asteroidal materials. The high-pressure polymorphs of olivine, ringwoodite and wadsleyite, are also major components of terrestrial planet mantles.
In the context of planetary exploration, it is common to face the question of whether an observed material has been affected by shock metamorphism. Reflectance spectroscopy is one of the most widely-applied remote mineralogical and geochemical analysis methods, but interpretation of remote reflectance spectra requires spectral libraries of well-characterized materials. Owing to the generally small size of synthetic high-pressure minerals, and to the extreme heterogeneity of natural high-pressure assemblages, reflectance spectral data for ringwoodite and other high-pressure phases do not exist at present. Here, we show the first visible and near-infrared reflectance spectra of a high-pressure polymorph of olivine, ringwoodite. These measurements are directly applicable to telescopic, orbiter, and robotic exploration of silicate surfaces throughout the solar system.

We have measured the first reflectance spectra of ringwoodite and wadsleyite. We show that both high-pressure olvine polymorphs are spectrally distinct from other ferromagnesian silicates. Ringwoodite samples were synthesized by first sintering a natural olivine powder (San Carlos olivine, $Mg_{1.8}Fe_{0.2}SiO_4$) in a piston-cylinder apparatus at 1.5 GPa and 1300 ºC, the pre-sintered material was then loaded in a Pt capsule and compressed to 20 GPa at 1500K in the Kawai-type 5000 ton multianvil press at IPM to convert the olivine to ringwoodite.

Ringwoodite reflectance spectra were acquired using a pair of imaging spectrometers: HySpex SWIR640 (400-1000 nm, 1800 pixels) and HySpex VNIR1800 (960-2500 nm, 640 pixels). Illumination was provided by two arrays of off-axis ~30º phase angle) 150 W quartz-tungsten-halogen bulbs. Nominal working distance was 30 cm. Wavelength calibration is made using HoO-doped spectralon (Avian Technologies). Hyperspectral data are converted from radiance to reflectance using a 100% reflectance diffuse spectralon target. This instrumentation allows reflectance spectra to be acquired even for the tiny (10s to 100s of microns) high-pressure synthesis charges investigated here.

The visible to near-infrared (VNIR) reflectance spectrum of ringwoodite is dominated by a broad feature near 800 nm, while the shortwave infrared (SWIR) reflectance spectrum shows a broad absorption centered near 1050 nm with a possible shoulder or inflection near 1200 nm. These features are ascribed to crystal field transitions of Fe^{2+} in octahedral coordination ($^5T_{2g} \rightarrow {}^5E_g$). Very weak features may be present near 1900 nm and 2300 nm, which could be ascribable to OH combination modes, an exciting possibility given that ringwoodite is well-known to incorporate significant H, but contamination cannot yet be ruled out. The spectral signature of ringwoodite is distinct from olivine (and pyroxene), which could enable the remote detection and characterization of ringwoodite-bearing materials, for example, in highly shocked materials within lunar or martian impact craters, or shocked ultramafic exposures on Earth. Further work is required to test the effects of chemical variations (e.g., Fe/Mg ratio, Fe3+/total Fe, hydration) on ringwooodite spectral signatures, as has been done with other rock-forming minerals. Other high-pressure phases should also be subjected to similar studies.

CARBONATE MELTS IN THE LITHOSPHERE-ASTHENOSPHERE BOUNDARY: GEOCHEMICAL EVIDENCE FROM ULTRAMAFIC XENOLITHS IN AN OCEANIC ISLAND

H. Kitagawa[1], T. Rooney[2], T. Ota[1], and T. Kunihiro[1],

[1] Institute for Planetary Materials, Okayama University (kitaga-h@cc.okayama-u.ac.jp), [2] Dept. of Earth and Environmental Sciences, Michigan State University (rooneyt@msu.edu).

Plate tectonics is one of the most important theories in Earth science, as it explains variable phenomena in geologic processes (e.g., earthquake and volcanism). This theory relies on mechanical coupling/decoupling of lithosphere (rigid plate) and asthenosphere (ductile region in the mantle); plates move over the mantle like drifting boats. In details, plate movement is facilitated by fluids acting as a "lubricant" at the lithosphere-asthenosphere boundary (LAB) [1]. It has been proposed that such fluids are produced by low-degree partial melting of asthenospheric mantle [2]. Such low-degree partial melts contain significant amounts of carbonate components [3]. Melts rich in carbonate components have low viscosity and high wetting capacity [4]. Mantle rocks containing such melts show high electrical conductivity [5]. The LAB, particularly in the vicinity of hotspots, often corresponds to zones of reduced seismic wave velocity and elevated electrical conductivity [6], suggesting the presence of carbonate melts. However, magmas with significant carbonate components, such as carbonatites, are rarely observed in modern oceanic volcanic settings. Carbonate melts are highly reactive with silicate minerals in the mantle; consequently, they are likely to be consumed via melt-rock interactions during ascent. The reaction involves the dissolution of low-Ca pyroxene and the precipitation of olivine, with or without high-Ca pyroxene [7]. This reaction produces specific lithologies, namely dunite and wehrlite [6, 7]. This, in turn, suggests that the coexistence of dunite and wehrlite serves as robust evidence for the presence of carbonate-bearing melts at depth. In this study, we investigated a suite of ultramafic xenoliths composed of dunite and wehrlite (Figure 1), collected from Faial Island in the Azores Archipelago. Notably, the host lavas are mildly alkaline rocks and do not contain significant carbonate components. Also noted is the complete absence of lithologies containing low-Ca pyroxenes, such as lherzolite and harzburgite, in the suite. For these xenoliths, in-situ chemical analyses were performed using electron probe micro-analysis (EPMA) and secondary ion mass spectrometry (SIMS). Major element compositions, of the primary phases (olivine, high-Ca pyroxene and Cr-spinel), determined by EPMA, indicates their mantle origins. Thermobarometric calculations [8] yielded 0.9–1.4 GPa (30–50 km), supporting their derivation from near the LAB (c. 45 km [9]). We identified the occurrence of two minerals that are rarely found in common mantle rocks: Ca-rich olivine (monticellite) and Al-rich clinopyroxene (fassaitic pyroxene). The formations of these minerals are attributed to reactions involving carbonate melts and mantle rocks [10, 11]. Preliminary SIMS analysis of these minerals reveals a significant enrichment in incompatible trace elements (e.g., Ba, Sr and rare earth elements). Such distinct geochemical signatures are likely inherited from the interacting carbonate-bearing melts [12], supporting the existence of carbonate-bearing melt at the LAB beneath Faial Island.

Figure 1. (left) dunite, (right) wehrlite

References: [1] Hua, J. et al. (2023) Nat. Geo., 16, 175–181. [2] Hirschmann, M. M. (2010) Phys. Earth Planet. Int., 179, 60–71. [3] Dasgupta, R. & Hirschmann, M. M. (2006) Nature 440, 659–662. [4] Hunter, R. H. & McKenzie, D. (1989) Earth Planet. Sci. Lett., 92, 347–356. [5] Yoshino, T. et al. (2010) Earth Planet. Sci. Lett., 295, 593–602. [6] Blatter D. et al. (2022) Nature, 604, 491–494. [7] Pintér et al. (2022) Commun. Earth Environ. 3, 296. [8] Neave, D. A. & Putirka, K. D. (2017) Am. Min. 102, 777–794. [9] Spieker, K. et al. (2018) Geophys. J. Int. 213, 824–835. [10] Dalton, J. A. & Wood, B. J. (1993) Earth Planet. Sci. Lett., 119, 511–525. [11] Kopylova, M. G. et al. (2021) Lithos, 388/389, 106045. [12] Green, D. H. & Wallace, M. E. (1988) Nature, 336, 459–462.

HYDROLOGY ON ANCIENT MARS DERIVED FROM MORPHOLOGIES AND TANK EXPERIMENTS OF DELTAS

R. Kito[1] and H. Hasegawa[2], T. Ruj[1], T. Muto[3], G. Komatsu[4]

[1] IPM, Okayama Univ. (Yamada 827, Misasa, Tottori 682-0193, Japan; rkito@s.okayama-u.ac.jp), [2] Kochi Univ. (Akebono-cho 2-5-1, Kochi, Kochi 780-8520, Japan), [3] Center for Public Relations Strategy, Nagasaki Univ. (Bunkyo 1-14, Nagasaki 852-8521, Japan), [4] Planetary Exploration Research Center, Chiba Institute of Technology. (Tsudanuma 2-17-1, Narashino, Chiba 275-0016, Japan.)

Several evidence of ancient aqueous environments has been found on the Martian surfaces such as outflow channels and valley networks and delta landforms. However, the hydrologic history of Mars remains debated, with interpretations ranging from a long-lived global ocean to spatially and temporally isolated lacustrine environments [1, 2]. Although Martian deltas are widely recognized as key indicators of surface water activity, the relationship between delta morphology and hydrologic regime has not been clearly established [3].

In this study, we show that Martian deltas record water-level fluctuations and transitions in surface hydrology. Using controlled laboratory tank experiments in which sediment supply and the rate of water-level change were held constant, we isolate the geomorphic responses to water-level rise and fall. These experiments identify two distinct depositional morphologies: 'lobe-extruding deltas (having elongated lobes)' formed during water-level falls and 'stepped fan deltas (having terraced topography)' formed during rising water levels. Previous experimental studies involved fluctuating discharge rates and water level changes due to erosion in the hinterland and infiltration into basins [4, 5]. However, the experimental design isolates the effect of water level changes alone.

Applying this experimentally derived framework to Mars, we mapped and classified deltas using orbital imagery and estimated their ages using crater size-frequency distributions (CSFD). The lobe-extruding deltas are located in plains at elevations ranging from approximately -2100 to -3120 m, and are clustered along the inferred coastlines [6]. Formation ages of these are indicated during ~3.8–3.2 Ga. These results suggest lobe-extruding deltas were developed during global ocean regression during the Hesperian. In contrast, stepped fan deltas are located in closed basins at wide elevation range (+1950 to -4670 m). Formation ages of these are indicated during ~3.5–0.1 Ga and peak during ~2.0-0.1 Ga. These results suggest stepped fan deltas were developed under isolated, short-lived lacustrine environments during the Amazonian. In addition, the orientation of river inflow that forms lobe-extruding deltas predominantly exhibit eastward to northward to flow. This is consistent with drainage into a northern ocean. In contrast, the orientation of river inflow that forms stepped fan deltas exhibit various directions, often trending southward. This supports localized hydrological processes. Additionally, we could not identify any deltas between 3.2-2.0 Ga, despite the continued presence of alluvial fans [7-10]. It implies that, although runoff was sufficient to construct alluvial fans during this interval, water volumes were inadequate to produce persistent crater lakes. Alternatively, warm episodes associated with volcanically driven meltwater may have been short-lived, with rapid reversion to cold and dry conditions that precluded long-term water storage and the development of stepped fan-deltas. The lack of deltaic activity points to a prolonged hydrological hiatus (~3.2–2.0 Ga) during which Mars transitioned into a much drier and colder climate. This interpretation is consistent with the decline of volcanism and fluvial erosion, global cooling, and the inferred collapse of Mars' early atmosphere, which would have limited the persistence of surface water [11-13].

Together, these results support a two-stage hydrologic evolution of Mars, from an early ocean-dominated system to later localized lacustrine environments and demonstrate that delta morphology provides a process-based record of planetary-scale hydrologic change. This framework offers new constraints on the evolution of Mars' paleoclimate and the persistence of surface water into the Amazonian.

Reference: [1] Di Achille, G. & Hynek, B. (2010) Nat Geosci 3, 459–463. [2] Rivera-Hernández, F., & Palucis, M. C. (2019) Geophys Res Lett, 46(15), 8689-8699. [3] De Toffoli, B. et al. (2021) Geophys Res Lett 48. [4] Kraal, E. R. et al. (2008) Nature, 451(7181), 973-976. [5] de Villiers, G. et al. (2013) Journal of Geophysical Research: Planets, 118(4), 651-670. [6] Sholes, S. F. et al. (2021) Journal of Geophysical Research: Planets, 126(5), e2020JE006486. [7] Morgan, A. M. et al. (2022) Icarus, 385, 115137. [8] Grant, J. A., & Wilson, S. A. (2011) Geophys Res Lett, 38(8). [9] Howard, A. D. et al. (2021) Icarus, 360, 114356. [10] Morgan, A. M. et al. (2014). Icarus, 229, 131-156. [11] Kite, E. S. et al. (2022) Science Advances, 8(21), eabo5894. [12] Warner, N. et al. (2009) EPSL, 288, 58-69. [13] Wordsworth, R. D. (2016) Annual Review of Earth and Planetary Sciences, 44, 381-408.

Tetrahedral symmetry breaking in albite-anorthite glass structures related to Aluminum atom: Possible origin of viscosity difference in plagioclase melts

N. M. Kondo[1], Y. Kono[2], K. Ohara[3], R. Nakada[4], [5]F. Noritake

[1]Institute for Planetary Materials, Okayama University (Yamada 827, Misasa, Tottori 682-0193; nozomikondo@okayama-u.ac.jp), [2] Kwansei Gakuin University (Kamigahara 1, Sanda-shigakuenn, Hyogo 699-1330), [3]Shimane University (Nishikawatsu-cho 1060, Matsue, Shimane 690-8504), [4]Kochi Institute for Core Sample Research (Monobe Otsu 200, Nankoku City, Kochi 783-8502), [5]University of Yamanashi (Takeda 4-4-37, Kofu, Yamanashi 400-8501)

Plagioclase is one of the major components in silicate melts, and albite [Ab] ($NaAlSi_3O_8$) and anorthite [An] ($CaAl_2Si_2O_8$) are endmembers of plagioclase solid solution. To understand transport property of silicate melts in the planetary interiors, investigation into physical properties and structures of Ab-An melts is essential. Many previous studies argued that viscosity of silicate melts is largely controlled by proportion of T(Si, Al)-O tetrahedra and non-bridging oxygen (NBO) in silicate melts (NBO/T = (2O-4T)/T, e.g. in[1]). In this NBO/T model, Ab melt and An melt should have similar viscosity, because they have the same value of NBO/T = 0. However, viscosity of An melt is 3-4 orders of magnitude lower than that of Ab at the same temperature and room pressure (e.g., [2]). Furthermore, viscosities of plagioclase melts are related to the proportion of Ab and An components, that is, the melt viscosity decreases with increasing An component. Therefore, the viscosity of plagioclase melts cannot be explained by the NBO/T model, and an exact mechanism governing the viscosity of plagioclase melts is still unknown.

In this study, we investigated structure of Ab-An glasses (quenched melts; compositions of Ab, An20, An40, An50, An60, An80, and An100) with high-energy X-ray diffraction and X-ray absorption to find structural difference related to An component. Glasses with Ab component (Ab, An20, An40, An50, An60, An80) were synthesized by an electric furnace at 1500-1700 ℃. Anorthite glass was synthesized by a levitation furnace with CO_2 laser at 1800-1900 ℃. The High-energy X-ray diffraction measurements were conducted at BL04B2 beamline at Spring-8, and the X-ray absorption measurements were conducted at BL27SU beamline at Spring-8.

From high-energy X-ray diffraction data, we did Pair Distribution Function (PDF) analysis and Molecular Dynamics-Reverse Monte Carlo (MD-RMC) analysis. As a result. intermediate scale structure of Ab-An glasses markedly change with An component. In Ab glass, the first and second shells of T atom showed ordered structure. We used parameter z ($z = \delta_{ji}-\delta_{j'i}$, where δ_{ji} and δ_{ji} are distance from a T atom (i) to the fifth nearest T atom (j) and to the fourth nearest T atom (j'), respectively), and z distribution of Ab glass shows peak at around 2.6 Å. With increasing An component, the z distribution shows bimodal peaks at around 2.6 Å and 1.5 Å. This bimodal feature of z distribution suggests collapse of the T atom second shell to the first shell (e.g., [3]). The MD-RMC models showed that Al can play essential role on the tetrahedral symmetry breaking. From X-ray absorption measurements, we conducted X-ray Absorption Near Edge structure (XANES) analysis, and investigated structural change related to Si, Al, and O. As a result, Al and O XANES spectra showed systematic change with An component. This result may suggest coordination change of Al related to An component. For Si XANES spectra, changes in Ab-An glasses are relatively smaller than Al. Therefore, Al atom would play important role on structural change in Ab-An glasses. From Ab to An composition, the glass structure shows transitional change from ordered to disordered feature. Such a structural change would be important to understand the viscosity difference in plagioclase melts.

References: [1] Mysen et al. (1980) Am. Min., 65 (11-12), 1150-1165. [2] Russell and Giordano (2005) GCA, 69(22), 5333-5349. [3] Kono et al. (2022) Nature Comm., 13(1), 2292.

SEARCHING FOR CLUES ABOUT THE EARLY IRON HISTORY IN CENTRAL ANATOLIA

N. Kucukarslan[1], T. Ota [2], C. Potiszil [2], K. Kobayashi [2], K. Matsumura [3], and S. Omura [3]

[1]Chiba Institute of Technology, Institute for Geo-Cosmology, Chiba, Japan, [2]Pheasant Memorial Laboratory for Geochemistry and Cosmochemistry, Institute for Planetary Materials, Tottori, Okayama University, Japan, [3]Japanese Institute of Anatolian Archaeology of the Middle Eastern Culture Centre in Japan, Kırşehir, Türkiye

Iron began to be widely produced in Central Anatolia during the Middle–Late Iron Age (ca. 900–430 BC) [1, 2]. However, ancient textual sources, including the Hittite records (ca. 1700–1200 BC) and earlier Assyrian trade documents [3, 4], suggest that knowledge of iron may have existed several centuries earlier. However, archaeological evidence for early iron production remains limited, and the timing of its emergence continues to be debated. At Kaman-Kalehöyük (Central Anatolia, Türkiye), a group of iron-rich artefacts was recovered from stratigraphic layers dated to the Early Bronze Age (ca. 2100–1930 BC) and Middle Bronze Age (ca. 2000–1400 BC). The assemblage includes iron-rich stones, slag fragments, and iron object fragments. This study thus explores whether iron production was available during these early periods.

The samples were examined using optical microscopy, FE-SEM equipped with EDS, and Raman spectroscopy. The results of SEM-EDS analyses on the artefacts indicate low Ni and Co concentrations, rarely up to 0.49 and 1.79 wt.%, respectively, and mostly below detection limits of the instrument. No Widmanstätten structures or other meteoritic phases were identified, suggesting that the artefacts are unlikely to originate from meteoritic iron. In addition, the SEM-EDS results of the slag samples show very low Cu concentrations, mostly below detection limits, and no Cu-bearing phases. It is thus unlikely that the slags were formed after copper production.

Microstructural observations of the slag samples revealed partially reacted ore grains within the glassy silicate matrix. In some cases, these ore-related grains are surrounded by a corroded iron phase, and small metallic iron relics are locally preserved. In addition, the results of the SEM–EDS and Raman analyses identified lamellar structures with higher carbon content than the surrounding matrix. These lamellar features were recognized as pearlite remnants, while the associated reduced iron is completely corroded. Although metallic iron is not preserved, the presence of pearlite remnants indicates former iron and steel formations up to ~5 mm in size within the slag samples.

All these findings suggest that technological conditions sufficient for iron production may have been achieved during the Early and Middle Bronze Ages in central Anatolia, possibly on a limited scale. Ongoing research aims to further constrain smelting temperatures and furnace atmosphere conditions to better understand the technological processes involved.

[1] Erb-Satullo, N. (2019) J. Archaeol. Res., 27, 557–607. [2] Masubuchi M. (2017) AAS, XX, 51-62. [3] Siegelova, J. And Tsumoto, H. (2011) In: Genz, H., Mielke D.P (eds.) Insights into Hittite History and Archaeology, 275-300. [4] Veenhof, K.R. (2016) Bibl. orient. 73(1-2), 14-40.

MINERALOGICAL HOSTS OF Be AND B IN RYUGU: IN SITU ION IMAGING CONSTRAINTS

N. Miklusicak[1] and T. Kunihiro[1],

[1]Institute for Planetary Materials, Okayama University, Misasa, Tottori 682-0193, Japan (tkk@misasa.okayama-u.ac.jp).

Bulk analyses of samples returned from the C-type asteroid Ryugu revealed a pronounced negative correlation between Be and B concentrations [1]. This relationship cannot be explained by volatility-driven fractionation or simple aqueous redistribution and instead implies the presence of chemically distinct carriers. However, the mineralogical hosts of Be and B in Ryugu have remained unidentified.

We conducted in situ SIMS ion imaging of a polished section of Ryugu particle C0027 to determine the microscale distribution of ^{9}Be and ^{11}B. The Be ion map reveals discrete, micrometer-scale domains sharply localized within a Be-poor background. In contrast, B is diffusely distributed and shows no spatial correlation with Be.

Electron microscopic observations demonstrate that the Be-rich domains correspond to euhedral Cr-rich oxide grains (chromite) associated with dense phyllosilicate nodules. Despite their extremely low modal abundance (~0.03 vol%), these oxides host a significant fraction of the total Be in the analyzed particle. Boron, by contrast, is predominantly hosted by phyllosilicates forming both the matrix and the interiors of the nodules.

The spatial decoupling of Be and B at the micrometer scale demonstrates that they reside in distinct mineral reservoirs. Because Be is concentrated in a rare Cr-rich oxide phase whereas B is distributed in volumetrically dominant phyllosilicates, the bulk Be–B anticorrelation observed in Ryugu cannot be reproduced by parent-body aqueous alteration alone. Instead, the Be–B systematics most likely reflect inheritance from precursor materials that experienced Be–B fractionation prior to asteroidal accretion.

References: [1] Nakamura E. et al. (2022) Proc. Jpn. Acad. Ser. B, 98, 227–282.

Systematic investigation of matrix effects in SIMS lithium isotope analysis: Constraints from the compositional dependence of in-house silicate standards

T. Moriguti[1,*] and T. Ota[1],

[1]Institute for Planetary Materials, Okayama University, Misasa, Tottori, Japan.
[*]moriguti@misasa.okayama-u.ac.jp

Lithium has unique physicochemical properties that make it a powerful tracer of planetary processes. These include: (1) its occurrence as a trace element in most rocks and minerals, (2) its high solubility in fluids, and (3) the significant relative mass difference between its two stable isotopes (^{6}Li and ^{7}Li), which results in large isotopic fractionations. As a pioneering study, Moriguti and Nakamura [1] demonstrated that lithium isotopes are an excellent geochemical tracer for understanding crust-mantle recycling at subduction zones. Since then, lithium isotopes have been widely applied to diverse geo- and cosmochemical processes, ranging from the earliest evolution of the solar system [e.g., 2] to global material recycling [e.g., 3, 4] and the evolution of liquid water on the surface of Mars [e.g., 5].

To decode these high-resolution in-situ isotope signatures, however, instrumental mass fractionation (IMF) in SIMS must be precisely corrected, as it arises from the fundamental physics of sputtering and ionization [e.g., 6, 7]. In lithium isotope analysis, the IMF is primarily governed by the matrix's chemical composition, as extensively described by Bell et al. [8], who established a linear correlation between Mg# and δ^{7}Li in olivine (approx. 1.3‰ per Mg# unit). While significant crystallographic orientation effects have been highlighted in oxygen isotopes [9], such effects in lithium are minimal or within analytical uncertainty [10]. According to a recent comprehensive review [11], compositional dependence remains the most critical factor for accurate matrix correction in silicate minerals.

In previous studies, however, a systematic evaluation of matrix effects across diverse silicate groups remains limited. In this study, we investigated these effects by utilizing an extensive set of silicate standards, including olivines, clinopyroxenes, garnets, and synthetic basaltic glasses. The bulk Li contents were determined by Q-ICP-MS [12], and the bulk δ^{7}Li values were precisely characterized using TIMS and MC-ICP-MS, following the established methods of Moriguti and Nakamura [13, 14] and Tang et al. [15]. In this presentation, we report the observed matrix effects in relation to chemical composition and discuss the homogeneity of these standard materials, providing a robust framework for high-precision in-situ Li isotope geochemistry.

References: [1] Moriguti T. and Nakamura E. (1998a) Earth Planet. Sci. Lett., 163, 167–174. [2] Teng F. Z. et al. (2023) Nat. Commun., 14, 3102. [3] Marschall H. R. et al. (2021) Geochim. Cosmochim. Acta, 293, 19–41. [4] Bebout G. E. et al. (2022) Geosphere, 18, 1020–1029. [5] Dellinger M. et al. (2021) Earth Planet. Sci. Lett., 573, 117031. [6] Slodzian G. et al. (1980) J. Phys. Lett., 41, 555–558. [7] Eiler J. M. et al. (1997) Chem. Geol., 138, 221–244. [8] Bell D. R. et al. (2009) Chem. Geol., 258, 82–95. [9] White L. F. et al. (2021) Chem. Geol., 583, 120404. [10] Zhang T. L. et al. (2015) J. Anal. At. Spectrom., 30, 368–377. [11] Li W. et al. (2023) J. Anal. At. Spectrom., 38, 1962–1969. [12] Moriguti T. et al. (2004) J. Anal. At. Spectrom., 19, 446–450. [13] Moriguti T. and Nakamura E. (1993) Proc. Japan Acad., 69B, 123–128. [14] Moriguti T. and Nakamura E. (1998b) Chem. Geol., 148, 1–9. [15] Tang Y. J. et al. (2007) Geochim. Cosmochim. Acta, 71, 4730–4740.

RECENT PROGRESS IN LUNAR SEISMOLOGY: DISCOVERY OF REPEATING SHALLOW MOONQUAKES IN THE APOLLO LUNAR SEISMIC DATA

K. Onodera[1]

[1] Institute for Planetary Materials, Okayama University, Misasa, Tottori, Japan
(konodera@okayama-u.ac.jp)

Seismic activity on the Moon serves as a crucial clue to understanding present-day tectonism [1-2]. Among the reported moonquakes, shallow moonquakes have been considered unique due to their large magnitudes and affinities to intraplate earthquakes [2-4]. However, the small number of detections has prevented detailed characterizations, making shallow moonquakes the most enigmatic seismic events on the Moon [2]. Here, I report a novel nature of shallow moonquakes revealed through an investigation of a recently renewed moonquake dataset that includes a threefold number of shallow moonquakes compared to the previous catalog [2, 5].

The main topic of this study is “repeating quakes”, that is, quakes repeatedly occurring at a given source. Such quakes are commonly observed on Earth, contributing to understanding fault physics and the processes of stress or strain accumulation. Also on the Moon, repeating moonquakes were reported. For example, deep moonquakes are known to correlate with tides and periodically occur depending on the orbital configuration of the Earth, Moon, and Sun system [6-8]. It is known that some deep moonquakes share the same source, called ``nest", and seismic signals radiated from a certain nest and recorded at the same station show similar features. On the other hand, there is no report about “repeating shallow moonquakes” since the first detection of shallow moonquakes in 1974 [9], even though shallow moonquakes are considered to be of tectonic origin and counterparts of intraplate earthquakes, which are plausible features to drive repeating events.

In this study, a quantitative evaluation of signal similarity between shallow moonquakes allowed me to discover a pair of repeating shallow moonquakes. Also, investigating the relationship between the lunar tidal phase and the relative polarity of seismic signals (i.e., relative fault slip direction), it turned out that they showed equal polarity even though they occurred in the opposite tidal phases. This implies that the tidal stress raised by the Earth and the Sun does not play a dominant role in initiating fault slips of the repeating shallow moonquakes, unlike deep moonquakes. With these results, it might be reasonable to think that these shallow moonquakes are attributed to the random stress release in the crust/upper mantle as previously proposed [1-2].

In addition, I also found that the repeating shallow moonquakes exhibit fault-physical relationship (slip scale vs. seismic moment) similar to that of typical earthquakes. Due to the small number of detections, shallow moonquakes are considered to be atypical and unique events on the Moon. However, in terms of fault physics, they appear to share more similarities with typical earthquakes than any other lunar seismic events. Since the driving force is different between Earth and the Moon, shallow moonquakes should not be entirely identical to earthquakes. Still, my results indicate that shallow moonquakes may be analogous to typical earthquakes, and that similar fault physics is at work on other solid planetary bodies.

In the presentation, I will outline the fundamental idea for identifying repeating quakes and showcase the discovered repeating events along with relevant fault parameters. Then, I will discuss the contribution of tides to the excitation of shallow moonquakes and provide implications for present-day lunar tectonics and affinities to earthquakes.

References: [1] Nakamura (1980), *Proc. LPSC*, XI, 1847-1853. [2] Onodera (2024), *JGR: Planets*, 129, 7, e2023JE008153. [3] Goins et al. (1981), *JGR: Solid Earth*, 86, B1, 378-388. [4] Oberst (1987), *JGR: Solid Earth*, 92, B2, 1397-1405. [5] Nakamura et al. (1981), *UTIG Technical Report*, No. 118. [6] Lammlein et al. (1974), *Reviews of Geophysics*, 12, 1, 1-21. [7] Nakamura (1978), *Proc. Lunar Planet. Sci. Conf.*, IX, 3589-3607. [8] Weber et al. (2009), *JGR: Planets*, 114 (E5). [9] Nakamura et al. (1974), *Proc. Lunar Planet. Sci. Conf.*, V, 3, 2883-2890.

HABITABILITY OF BORON-RICH ENVIRONMENT IN ANCIENT SEA; INSIGHTS FROM TOURMALINE IN A MESOARCHEAN PELAGIC HYDROTHERMAL SYSTEM

T. Ota [1], S. Kiyokawa[2], and R. Tanaka[1]

[1] Pheasant Memorial Laboratory for Geochemistry and Cosmochemistry, Institute for Planetary Materials, Okayama University, Misasa, Tottori 682-0193, Japan. e-mail: ohta-t@misasa.okayama-u.ac.jp
[2] Department of Earth and Planetary Sciences, Kyushu University, Fukuoka 813-8581, Japan.

The RNA world hypothesis requires the synthesis of RNA to allow the emergence of life on Earth. Hydrothermal systems have been proposed as potential candidates for constructing complex biomolecules. However, in order to successfully form RNA, it is necessary to stabilize ribose, a RNA carbohydrate component. Borate has been found to stabilize ribose. Therefore, boron rich hydrothermal systems are important environments concerning the origin of life on Earth.

The 3.2-Ga Dixon Island Formation of the West Pilbara Superterrane, Western Australia, is a volcano-sedimentary sequence. The Formation represents a Mesoarchean pelagic hydrothermal system, which formed adjacent to an immature island arc. Fine-grained tourmaline, in addition to biogenic carbonaceous matter and spherulitic and tubular bacteriomorphs, are found in black chert. A boron-rich environment was responsible for the formation of these deposits. To explore the implications of such a boron enriched environment on microbial activity, modes of occurrence and chemical compositions of the tourmaline were examined [1].

The tourmaline is schorl or dravite of the alkali tourmaline group and the boron isotope compositions range in $\delta^{11}B$ from –7.3 to +2.6 ‰. The tourmaline occurs in microcrystalline quartz matrix of black chert veins that crosscut a volcanic unit, and also in a bedded black chert, which overlays the volcanic unit. The volcanic unit contains highly altered zones with hydrothermal veins. The associated lithologic and stratigraphic features suggest that the black chert veins were the conduits for upward moving hydrothermal fluids, which reached the sea floor. Subsequently, the volcanic unit was covered by organic matter-rich cherty sediments that in part were fed, and/or altered, by the hydrothermal fluids.

These results suggest that the origin of boron enrichment to form Dixon Island tourmaline is not the associated sedimentary mineral assemblage, which includes diagenetic clay, low-grade metamorphic mica, and organic matter. Instead, the tourmaline was directly precipitated from hydrothermal fluid, enriched in boron. Furthermore, the hydrothermal fluids had already concentrated the boron enough to form the tourmaline by seawater circulation in oceanic crust in the Mesoarchean pelagic system, prior to the apex of organic matter production and microbial activity. This implies that boron-enriched hydrothermal environments such as geysers and other terrestrial hydrothermal systems [2, 3] could have existed also on the ocean floor in the Hadean and the early Archean times, when terrestrial land mass has been limited.

Our findings support a hypothesis that the boron-enriched hydrothermal environment aided the survival and evolution of early life.

References: [1] Ota, T., Aihara, Y., Kiyokawa, S., Tanaka, R., and Nakamura, E. (2019) Precambrian Research 334, 105475, doi: 10.1016/j.precamres.2019.105475. [2] Steller, L. H., Nakamura, E., Ota, T., Sakaguchi, C., Sharma, M., and Van Kranendonk, M. J. (2019) Astrobiology 19, 1459–1473, doi:10.1089/ast.2018.1966. [3] Van Kranendonk, M. J., Baumgartner, R., Djokic, T., Ota, T., Steller, L., Garbe, U., and Nakamura, E. (2021) Astrobiology 21, 39–59, doi: 10.1089/ast.2019.2107.

GEOCHEMICAL AND ISOTOPIC CHARACTERISTICS OF THE MAGNITOGORSK AND UI RIVER ZONES' EARLY CARBONIFEROUS VOLCANIC COMPLEXES (SOUTHERN URALS, RUSSIA)

N.V. Pravikova[1], H. Kitagawa[2], C. Sakaguchi[2], E. Kalinina[3], and A.V. Tevelev[1]

[1] Lomonosov Moscow State University, 1, Leninskie Gory, Moscow, 119991, Russia, natalia.v.pravikova@gmail.com; [2] Institute for Planetary Materials, Okayama University, 827 Yamada, Misasa, Tōhaku District, Tottori 682-0193, Japan; [3] Department of Comprehensive Technical Solutions, Okayama University, 3-1-1 Tsushima-naka, Kita-ku, Okayama City, Okayama 700-8530, Japan

Early Carboniferous volcanic rocks from the Magnitogorsk and Ui River zones of the Southern Urals provide critical insights into the transition from active subduction to post-collisional tectonics. We present new geochemical data to constrain magma sources and the role of crustal architecture during this transitional period.

The studied volcanics range from basalts to rhyolites. Mafic rocks are porphyritic with pyroxenes and plagioclase phenocrysts set in a fine-grained to microlitic groundmass. Felsic rocks range from porphyritic to aphyric rhyolites and ignimbrites, featuring fluidal textures, fiamme, and zoned feldspar phenocrysts, indicating contrasting cooling histories and magma storage conditions. Major element systematics define a differentiation trend from mafic parental melts to felsic derivatives, characterized by decreasing MgO, Fe_2O_3*, TiO_2, and CaO with increasing SiO_2, accompanied by enrichment in total alkalis, consistent with fractional crystallization dominated by early mafic mineral removal followed by extensive plagioclase fractionation.

Trace element patterns of the basaltic rocks show moderate enrichment in incompatible elements with pronounced negative Nb–Ta and positive Pb anomalies, reflecting inheritance from a subduction-modified mantle source. However, they lack systematic enrichment in fluid-mobile elements (Rb, Ba), indicating derivation from previously metasomatized lithospheric mantle rather than from active slab-fluid input. Flat HREE patterns suggest shallow, spinel-facies melting. Basalts from the Ui River zone exhibit greater variability in incompatible trace element concentrations than those from the Magnitogorsk zone, reflecting variable degrees of partial melting and/or source enrichment within a similar mantle.

Felsic rocks display highly fractionated trace element patterns with strong negative Ba, Sr, and Eu anomalies, consistent with extensive plagioclase-dominated fractional crystallization. Similar LREE/HREE fractionation in basaltic and felsic rocks supports a genetic relationship, with felsic magmas representing differentiated derivatives of mantle-derived melts rather than independent crustal melts.

Sr–Pb isotope systematics provide key constraints on magma evolution and crustal interaction. Basaltic rocks from both zones show uniform, mantle-like Sr isotope ratios and tightly clustered Pb isotope compositions, indicating minimal modification during magma ascent. In contrast, felsic rocks exhibit strong Sr isotope variability: Ui River felsic samples show uniformly radiogenic compositions, consistent with interaction with a homogeneous evolved continental crust, whereas Magnitogorsk samples display a wide range, implying assimilation of a compositionally heterogeneous crustal basement. The hyperbolic trend on $^{87}Sr/^{86}Sr$ vs. 1/Sr diagram indicates assimilation–fractional crystallization (AFC) processes during magma differentiation.

The combined geochemical and isotopic characteristics are best explained by magmatism in a post-subduction extensional setting. Lithospheric thinning or asthenospheric upwelling triggered partial melting of a previously metasomatized lithospheric mantle, producing basaltic melts with inherited arc-like signatures. Subsequent differentiation within continental crust led to variable crustal assimilation and generation of isotopically distinct felsic magmas. Differences between the zones likely reflect fundamental variations in crustal architecture and basement composition, marking a major crustal boundary within the Southern Urals. Our study thus reveals previously unrecognized crustal heterogeneity and provides new constraints on terrane architecture and the tectonic evolution of the Southern Urals.

Major element analyses for 7 samples were conducted in SU FRC MG UB RAS (Miass, Russia), and all remaining geochemical work was performed using the Comprehensive Analytical System for Terrestrial and Extraterrestrial Materials (CASTEM) at the PML, IPM, Okayama University at Misasa [1].

References: [1] Nakamura, E., Makishima, A., Moriguti, T., Kobayashi, K., Sakaguchi, C., Yokoyama, T., et al. (2003). Comprehensive geochemical analyses of small amounts (< 100 mg) of extraterrestrial samples for the analytical competition related to the sample return mission MUSES-C. Inst. Space Astronaut. Sci. Rep. SP., 16, 49–101.

Reconstructing the Martian Surface Environment Through Polygonal Patterned Ground

○Takaki Sako[1], Hitoshi Hasegawa[2], Trishit Ruj[1], Goro Komatsu[3,4], Noritaka Endo[5]
[1] IPM, Okayama University (Misasa 682-0193, Japan); E-mail: sakotaka@s.okayama-u.ac.jp, [2] Faculty of Science and Technology, Kochi University (Kochi 780-8520, Japan), [3] IRSPS, Università d'Annunzio (Pescara 65127, Italy), [4] PERC, Chiba Institute of Technology (Chiba 275-0016, Japan), [5] Kanazawa University (Kanazawa 920-1192, Japan)

Ancient Mars had abundant water, but the planet later became a cold and arid environment [1][2]. However, observations from the Phoenix Mars Lander, including temperature and humidity measurements and the detection of perchlorates, suggest that stable liquid brines could persist near the surface even in cold high-latitude environments [3].

To better understand Mars' liquid environment, this study focuses on desiccation polygons that may form due to liquid evaporation from the surface [4]. The supply and circulation of water from the subsurface control the formation and their morphology of these polygonal terrains [5][6]. This study proposes a paleo-hydrological framework based on the morphology between 'Raised rim' and 'Low rim' desiccation polygons. Utilizing a combined approach, we investigated the environmental drivers of polygon morphology. First, global terrestrial analog surveys were conducted using satellite data (ASTER, Sentinel-2) followed by field investigations in the Atacama Desert and the Western United States. Second, laboratory desiccation experiments were performed using bentonite clay and NaCl solutions to isolate the physical mechanisms of rim formation under controlled salinity and evaporation rates. Lastly, global mapping of Martian crater floor polygons was conducted using High-Resolution Imaging Science Experiment (HiRISE) imagery to identify spatial trends in morphology across various latitudes.

Terrestrial analog surveys using satellite data (via Google Earth, ASTER, and Sentinel-2) and field investigations in the Atacama Desert and the western United States, we show that Raised rim polygons are associated with sustained liquid activity and evaporite precipitation (including halite and gypsum), whereas Low rim polygons form under more limited liquid involvement, dominated by simple desiccation processes with minimal mineral accumulation.

Laboratory experiments using halite support these observations, demonstrating that Raised rim development requires both elevated salinity and relatively slow evaporation, whereas rapid drying or low salinity favors Low rim morphologies. This result shows Raised rim polygons are formed by stable high salinity condition.

Analysis of HiRISE images reveals that Raised rim polygons are dominant in polar regions (>60° latitude), while Low rim polygons prevail at mid to low latitudes. This distribution is consistent with brine stability models. These results provide evidence that Amazonian Mars also hosted localized brine activity, particularly in polar regions. Raised rim polygons along with lower crater density in the high latitude regions indicate geologically recent liquid-related processes. These areas could be high-priority targets for future explorations with potential biologic activity.

References: [1] Hynek, B. M., et al., JGR: Planets 115.E9 (2010). [2] Head, J. W., et al. Nature 426.6968 (2003): 797-802. [3] Rivera-Valentín, E. G., et al. Nat. Astro 4.8 (2020): 756-761. [4] El-Maarry, M. R., et al. *Icarus* 241 (2014): 248-268. [5] Vanden B., et al., The Sedimentary Record 17.1 (2019): 4-10. [6] Lasser, J., et al., Earth System Science Data 12.4 (2020): 2881-2898.

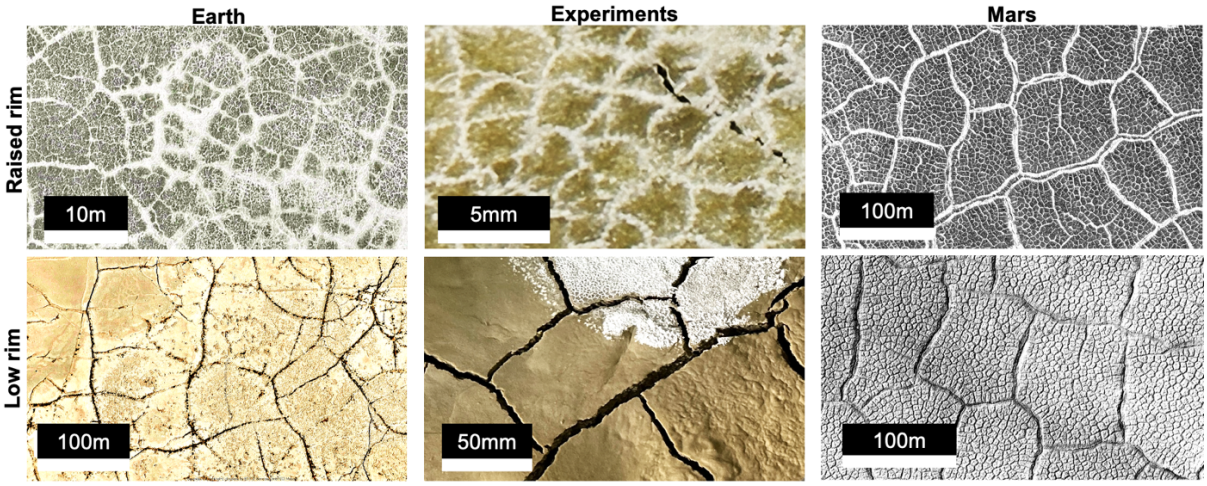

Fig. 1. Comparison of raised-rim and low-rim polygon morphologies across Earth analog sites, laboratory experiments, and Mars.

Exploring the aqueous environmental history of Eridania Basin on Mars

Karin Sugiura[1], Hitoshi Hasegawa[1], Trishit Ruj[2]

[1] Faculty of Science and Technology, Kochi University (Akebono-cho 2-5-1, Kochi 780-8520, Japan: e-mail: b253u010@s.kochi-u.ac.jp). [2] Institute for Planetary Materials, Okayama University (Yamada 827, Tottori 682-0193, Japan).

During early Noachian (~4.1–3.8 Ga), Mars thought to have an active core dynamo that generated a global magnetosphere, and surface conditions may have supported a warm and wet environment with extensive oceans, resembling present-day Earth. The Martian dynamo weakened or ceased by the late Noachian to early Hesperian (~3.7 Ga) [1]. Following this decline, Mars transitioned toward colder and drier surface conditions. However, the relationship between the disappearance of magnetosphere and the environmental change on the Martian surface remains poorly understood.

In this study, we focused on the Eridania region in the southern highlands of Mars, an area characterized by numerous water-related landforms such as chaotic terrains and desiccation-related polygons [2,3], evidence of hydrothermal activity [4], and strong remanent magnetic fields [5]. We explored geomorphological features and estimated formation ages of five sub-basins in the Eridania region: Ariadnes, Caralis, Atlantis, Simois, and Gorgonum.

Our results show that chaotic terrains and desiccation-related polygonal terrains are concentrated in the central areas of the five sub-basins, with model ages estimated to be 3.6 to 3.4 Ga. Previous study also suggest that surface aqueous activity persisted until late Hesperian (e.g., 3.3~3.2 Ga) [2,3]. These observations imply that aqueous environment may have continued on the Martian surface even after the loss of the magnetosphere, providing important insights into the environmental history of Mars.

References: [1] Ehlmann, B. L., *et al.* (2016) *JGR: Planets* 121.10: 1927-1961. [2] Adeli, S., *et al*. (2015) *JGR: Planets*, 120, 1774–1799. [3] Dang, Y., *et al*. (2020) *JGR: Planets*, *125*, e2020JE006647. [4] Michalski, J. R., *et al.* (2017) *Nature coms.* 8.1: 15978. [5] Connerney, J. E. P., *et al.* (2005) *PNAS* 102.42: 14970-14975.

Infiltration of Fe-S Melt into Ilmenite: Implications for the Lunar Low-Velocity Zone

H. Takaki[1] and T. Yoshino[1]

[1] Institute for Planetary Materials, Okayama University (Yamada 827, Misasa, Tottori 682-0193, Japan)

Seismic observations indicate the presence of a low-velocity zone (LVZ) at the base of the lunar mantle above the core–mantle boundary (CMB), where wave velocities decrease from ~8.5 to ~7.5 km/s in V_P and from ~4.5 to ~3.2 km/s in V_S [1]. This zone has commonly been interpreted as an ilmenite-rich partially molten layer formed after a mantle overturn event, during which dense ilmenite-bearing cumulates sank and accumulated near the CMB [2]. However, the estimated CMB temperature of ~1400 °C [3] raises questions about whether extensive partial melting of ilmenite-rich material is thermodynamically plausible under present lunar conditions.

Here, we propose that the LVZ may instead be related to Fe–S melt infiltration into an ilmenite-rich layer. The lunar outer core is estimated to contain approximately 10–20 at.% sulfur [4], implying the presence of Fe–S liquid at the base of the mantle. Because of the density contrast between Fe–S melt and surrounding mantle materials, simple porous percolation is unlikely to sustain melt transport over ~150 km, corresponding to the inferred thickness of the LVZ. Therefore, an additional mechanism is required to enhance melt infiltration. Morphological instability, which arises when two materials are not in overall chemical equilibrium and are separated by a chemical potential gradient, may modify melt pathways and facilitate localized, deeper infiltration beyond what is expected from simple porous flow [5].

To evaluate this hypothesis, we conducted high-pressure infiltration experiments between sintered ilmenite and $Fe_{60}S_{40}$ melt at 4.5 GPa and 1400 ºC. The results show that Fe–S melt readily infiltrates sintered ilmenite along grain boundaries. In natural single-crystal ilmenite, melt infiltration exhibits deep finger-like structures resembling morphological instability textures previously reported in ferropericlase systems [5]. These observations indicate that Fe–S melt can effectively infiltrate ilmenite-rich layers under lunar CMB conditions.

The presence of Fe–S melt within an ilmenite-rich layer may significantly reduce seismic velocities and could account for the observed decreases in both V_P and V_S without requiring ilmenite or silicate partial melting. Our results suggest that Fe–S melt infiltration into an ilmenite layer is a plausible mechanism for generating the seismic low-velocity structure at the base of the lunar mantle.

References: [1] Weber, C. W. et al. (2011) *Science*, 331, 309–312. [2] Zhao, Y. et al. (2019) *Earth Planet. Sci. Lett.*, 511, 1-11. [3] Khan, A. et al. (2006) *Earth Planet. Sci. Lett.*, 248, 579–598. [4] Antonangeli, D. et al. (2015) *PNAS*, 112, 3916–3919, [5] Otsuka, K. & Karato, S. (2012) *Nature*, 492, 243–246.

Method development of novel organic-inorganic interface molecules in the Solar System: Optimization and perspectives of hybrid cross-separation with high-resolution mass spectrometry

Yoshinori Takano[1,2]

1) Japan Agency for Marine-Earth Science and Technology (JAMSTEC), Yokosuka, Kanagawa 237-0061, Japan.
2) Institute for Advanced Biosciences (IAB), Keio University, Tsuruoka, Yamagata 997-0052, Japan.

A wide variety of organic compounds exist in the Solar System. Primordial records of chemical evolution in the asteroid Ryugu reveal over 200,000 organic mass signals, from which more than 20,000 molecular formulas have been assigned [1]. Among these evaluation, molecular evidence of keto-enol tautomerism due to hydrothermal alteration has also been identified [e.g., 2,3]. The molecular formula for alanine, a representative amino acid, is C_3H_7NO. Theoretically, chemical structures with this molecular formula include over 50 types when considering structural isomers (e.g., α-alanine: CH_3-$CH(NH_2)$-COOH, β-alanine: NH_2-CH_2-CH_2-COOH, and sarcosine: CH_3-NH-CH_2-COOH) and the enantiomers (D-, L-α-alanine). Therefore, accurate molecular structure assignment requires comprehensive cross-validation on non-targeted to targeted analysis. We optimized the hybrid separation techniques on the chromatography (LC/IC, GC) and electrophoresis (CE) utilizing polar and non-polar distribution, affinity with the stationary phase and wet-chemical treatments [2,4-6]. The cross-assessing development of high-resolution mass spectrometry has advanced our understanding of molecular diversity representing organic, inorganic, and complex molecular groups in nature [e.g., 4-6]. The asteroid Bennu is rich in nitrogen compounds (e.g., ammonia, amino acids, nucleobases [7]), and its water-extractable fraction was weakly alkaline (pH = 8.23 ± 0.02) [8]. The optimized methods will provide further important insights for comparative studies of organic chemical evolution on the two carbonaceous asteroid Ryugu [1-4] and Bennu [7-10].

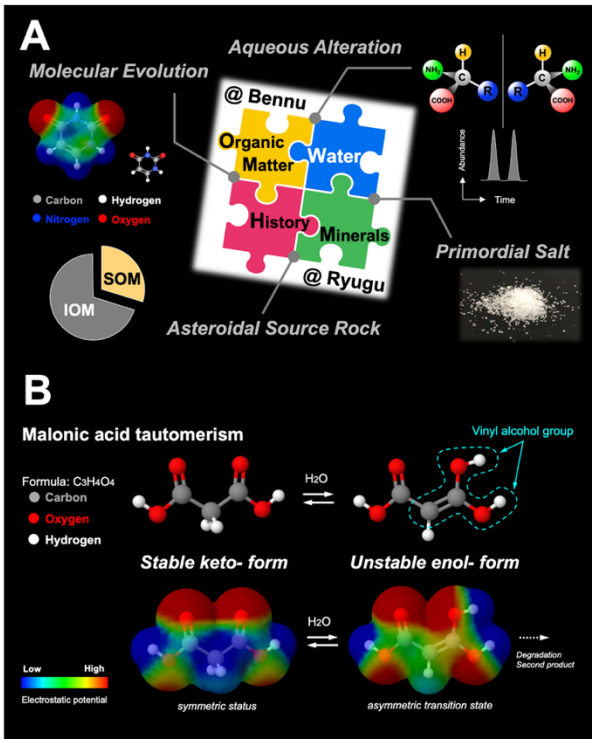

Figure 1. (A) Conceptualization of the chemical evolution, molecular chirality, and organic astrochemistry on the Ryugu protocol [illustration after 1-4, 5-10].
(B) The tautomeric isomerization of malonic acid (C_3-dicarboxylic acid) as an organic molecular indicator of aqueous alteration [2,10]. The electrostatic potential representing the intramolecular electron density is shown as color contours.

References: [1] Naraoka et al. Science 379, eabn9033 (2023). [2] Takano et al. Nature Commun. 15, 5708 (2024). [3] Oba et al. Nature Commun. 14, 3107 (2023).; Nature Commun. 14, 1292 (2023). [4] Yoshimura et al. Nature Commun. 14, 5284 (2023). [5] Hirakawa et al. ACS Omega 10, 42061–42067 (2025). [6] Koga et al. Geochim. Cosmochim. Acta 365, 253–265 (2024). [7] Glavin et al. Nature Astron. 9, 199–210 (2025) and following papers. [8] Furukawa et al. Nature Geosci. 19, 19–24 (2026). [9] Hirakawa et al. LPSC (2025); Koga et al. LPSC (2025). [10] Takano et al. Goldschmidt. doi: 10.7185/gold2025.29671 (2025).

DEVELOPMENT OF A VACUUM ULTRAVIOLET LASER FOR A THORIUM-229 NUCLEAR CLOCK

S. Takatori[1], M. Guan[1], T. Hiraki[1], T. Masuda[1], R. Ogake[1], K. Okai[1], N. Sasao[1], K. Shimizu[1], A. Yoshimi[1], and K. Yoshimura[1]

[1] Research Institute for Interdisciplinary Science (RIIS), Okayama University

Nuclear transitions are typically driven by X-rays or γ-rays. Thorium-229 is unique in that it is the only known nucleus expected to possess an excited state at an energy low enough to be accessed with vacuum-ultraviolet (VUV) laser light. A nuclear clock based on this unique transition is expected to become a next-generation high-precision frequency standard, with potential impact ranging from verifying from fundamental physics to practical applications in society. A major technical challenge is the realization of a VUV light source with sufficient intensity and stability at the required wavelength. In this work, toward direct laser excitation of thorium-229, we developed a pulsed VUV laser system based on frequency conversion via four-wave mixing. This presentation reports the VUV generation scheme, recent improvements, and key performance characteristics of the developed system.

Cryogenic Evaluation of Magnetic Field Characteristics in a Velocity-Type Passive Seismometer

Kazuki Yamanaka[1,2], Satoshi Tanaka[2], and Keigo Enya[2]

[1] SOKENDAI (The Graduate University of Advanced Science), [2] ISAS (Institute of Space Astronautical Science)

Seismic observations provide critical constraints on the internal structure and evolutionary processes of planets, including Mars. Future Japan-led Mars exploration missions are currently under consideration, where stable seismic monitoring in cryogenic environments—such as polar nights and high-latitude regions—will be essential.

Concurrently, JAXA is developing a velocity-type passive seismometer capable of operating at cryogenic temperatures for NASA's Dragonfly mission to Saturn's moon, Titan. This seismometer is also expected to be applied to the STEP1 mission, a new Mars exploration initiative. A key technical challenge for next-generation planetary seismology is ensuring the sensor's response characteristics under harsh thermal environments. This is particularly difficult because the permanent magnets within the sensor exhibit a significant increase in magnetic field strength at cryogenic temperatures. Therefore, characterizing the temperature dependence of the internal magnetic circuit is a vital task.

In this study, a magnetic field measurement probe using a micro-Hall element was developed to perform two-dimensional measurements of the flux density distribution within the magnetic gap at both room temperature and liquid nitrogen temperature (approx. 77 K). Due to restrictions on direct cryogenic testing of the Flight Model (FM) during ongoing qualification trials, the seismometer that served as the base model for the one on Dragonfly was used as a substitute. This model shares the same geometric structure and magnetic circuit design as the Dragonfly model. Preliminary room-temperature measurements confirmed similarity in the spatial distribution of flux density, with a gap dimension difference of only about 10%. Thus, the results of this experiment function as a scalable reference model for predicting the behavior of the Dragonfly model at cryogenic temperatures.

The experimental results revealed that while the average magnetic field strength in the gap increased by approximately 15%, the rate of increase was highly non-uniform spatially. Specifically, a sharp increase of 60–80% was recorded at the bottom of the gap, whereas the magnetic field strength switched to a decrease of up to 30% near the top. This indicates that the phenomenon is driven not only by the inherent changes in the permanent magnet's strength but primarily by the redistribution of magnetic flux within the circuit at cryogenic temperatures.

These findings highlight a significant risk: cryogenic environments can cause sensitivity non-uniformity that deviates drastically from room-temperature characteristics, potentially introducing non-linear distortions into observed waveforms. For future planetary seismic missions such as STEP1 and Dragonfly, calibrating response functions to account for these temperature-dependent magnetic profiles is an indispensable process for achieving high-precision observations.

Climate Control On Cr And Ni Bioavailability In Ultramafic Soils Along An Elevation Gradient In Mt. Kinabalu, Malaysia

Chia-Yu Yang[1], Atsushi Nakao[1], Sumika Kataoka[1], Rota Wagai[2], Shin-ichi Yamasaki[3], Junta Yanai[1], and Takashi Kosaki[4]

[1] Department of Life and Environmental Sciences, Kyoto Prefectural University, 1-5 Shimogamohangi-cho, Sakyo-ku, Kyoto, 606-8522, Japan (e-mail: cyyang@kpu.ac.jp), [2] Institute for Agro-Environmental Sciences, National Agriculture and Food Research Organization, 3-1-3 Kannondai, Tsukuba, 305-8604, Japan, [3] Graduate School of Environmental Studies, Tohoku University, Aramakiaoba 6-6, Aoba-ku, Sendai, 980-0845, Japan, [4] Faculty of International Communication, Aichi University, 4-60-6 Hiraike-cho, Nakamura-ku, Nagoya, 453-8777, Japan

Climate exerts a fundamental influence on soil chemical weathering, hydrological fluxes, and redox conditions, thereby regulating trace metal redistribution through pedogenic processes rather than total metal contents alone. Ultramafic soils are characterized by anomalously high concentrations of potentially toxic elements, particularly chromium (Cr) and nickel (Ni), compared to non-ultramafic soils, which can pose risks to ecosystem health and constrain plant establishment. In ultramafic soils, previous studies across broad climatic regions have suggested that Cr and Ni bioavailability varies systematically with climatic conditions and pedogenic stage. However, how elevation-driven climatic gradients regulate the behavior of Cr and Ni within a single ultramafic system remains poorly constrained. To address this knowledge gap, we investigated four ultramafic soil profiles located at 748, 1700, 2700, and 3100 m a.s.l. along an elevation transect on Mount Kinabalu, Malaysia. Mineralogical composition, physicochemical properties, soil classification, Fe speciation, plant available metal pools in soils, and plant uptake experiments were integrated to evaluate elevation-related pedogenic controls on Cr and Ni accessibility. Along the elevation gradient from the lowest to the highest site, the soils were highly weathered and oxidized red soils (Oxisols), well-developed soils (Ultisols), shallow and immature soils (Entisols), and humus-rich and weakly weathered soils (Inceptisols), respectively. Across the transect, Si–Mg–Fe compositions and Fe chemical species demonstrated that the lowest-elevation profile, KB1, exhibited the greatest depletion of Si and Mg and the highest relative proportion of Fe. In addition, KB1 was characterized by the lowest Fe (II)/total Fe ratio and the highest secondary Fe oxides amount. However, the proportions of Si, Mg, and Fe and the Fe species did not vary systematically with elevation. Chromium remained strongly retained across all profiles, with consistently low extractable concentrations and limited plant uptake, despite substantial variation in soil chemical and mineralogical properties. In contrast, Ni exhibited pronounced variability in extractable pools and root uptake, particularly in mid and high-elevation soils. These results indicated that elevation did not define a unidirectional pedogenic sequence but instead constrained chemical and biological pedogenic pathways that selectively regulated plant available metal pool.

Keywords: weathering index, elevation, Soil Taxonomy, soil development, plant uptake

Effect of Fe on electrical conductivity of wadsleyite: implications for conductivity structure of deep Martian mantle

T. Yoshino[1]

[1] Institute for Planetary Materials, Okayama University
e-mail: tyoshino@misasa.okayama-u.ac.jp

The seismic velocity structure of the Martian mantle has been significantly improved by the InSight mission [1,2], but the electrical conductivity structure remains poorly constrained. One feature of Martian mantle is its high iron content compared to the Earth's mantle. Therefore, the electrical conductivity of the Martian mantle is expected to be higher than that of Earth by small polaron conduction. The high-pressure polymorphs of olivine and the emergence of two-phase coexistence regions likely lead to a more complex mantle transition zone, resulting in a more complex electrical conductivity structure compared to Earth due to the different amounts of iron partitioned between the phases. However, the influence of iron on the electrical conductivity of wadsleyite, a key element of Martian mantle, has not been well constrained due to the very narrow temperature and pressure range over which single-phase wadsleyite is stable. In this study, we investigated the influence of iron on the electrical conductivity of wadsleyite by impedance spectroscopy at 16 GPa. Similar to olivine and ringwoodite, the electrical conductivity of wadsleyite increased with increasing iron content, while the activation enthalpy for electric conduction decreased. The electrical conductivity profile of the Martian mantle considering the two-phase region generally shows complex conductivity jumps across the regions of olivine-ringwoodite, olivine-wadsleyite, and wadsleyite-ringwoodite. We conclude that the electrical conductivity structure constructed based on the electrical conductivity measurements in this study is difficult to reproduce the model proposed based on observations showing large electrical conductivity jumps.

References: [1] Samuel H. et al. (2023) Nature, 612, 712–717. [2] Khan A. et al. (2023) Nature, 612, 718–723.